uc3m | Universidad **Carlos III** de Madrid

University Degree in Mechanical Engineering
2016/2017

Bachelor Thesis

Modeling and Optimization of a Heat Recovery Steam Generator (HRSG)

Author: Ángel Jesús García Frías

Tutor: Luis Miguel García Gutiérrez

Madrid, September 2017

Acknowledgments

To my family and friends.
They inspired me, gave me hope, strength and courage.
They made possible that this project came to a successful end.

Table of Contents

List of Figures

List of Tables

List of Equations

List of Symbols

Symbol	Units	Description
AP	K	Approach point temperature
$CCPP$	-	Combined cycle power plants
COT	-	Combustor outlet temperature
Cp	J/(mol kg)	Constant pressure specific heat
EC	-	Economizer
EV	-	Evaporator
F	-	Correction factor for ΔT_{lm}
HP	-	High pressure level
$HRSG$	-	Heat Recovery Steam Generator
H	J/kg	Specific enthalpy
IP	-	Intermediate pressure level
LP	-	Low pressure level
L_t	m	Length of tubes
M	kg/s	Mass flow
N_c	-	Number of columns of tubes
N_r	-	Number of rows of tubes
N_t	-	Total number of tubes
Nu	-	Nusselt number
PD	Pa	Pressure drop
PP	K	Pinch point temperature
P_m	Pa	Mean pressure
Pr	-	Prandtl number
P	Pa	Pressure
Re	-	Reynolds number
SH	-	Superheater
S_d	m	Diagonal pitch
S_l	m	Longitudinal pitch
S_t	m	Transverse pitch
TTD	-	Terminal temperature difference
T_m	K	Mean temperature
T	K	Temperature
UA	W/K	UA coefficient
U	W/(m^2 K)	Global heat transfer coefficient
X	-	Mass vapor quality
ΔT_{lm}	K	Log mean temperature difference
η	-	Efficiency
μ	Pa s	Viscosity
ρ	kg/m^3	Density
d_i	m	Inside diameter of tubes
d_o	m	Outside diameter of tubes
f	-	Petukov friction factor
g	-	Subscript for gas
h	W/(m^2 K)	Heat transfer coefficient
k	W/(m K)	Conductivity
s	-	Subscript for steam
v	m/s	Velocity

Abstract

The world is slowly changing the way energy is obtained. Recent trends are discovering that renewable energies are the future of the energy industry. However, they only represented 10% of the total primary energy sources around the world last year (2016). Present energy production processes need developments to compete with those new emerging technologies. Combined cycle power plants (CCPP) provide an efficient way of obtaining electricity, nevertheless, there is still room for improvement. This project is focused on the optimization of one of the most important elements in the cycle: the heat recovery steam generator (HRSG). A thermodynamic analysis will be performed along with other calculations. Results of this optimization show that it is possible to decrease the heat exchanged area of the HRSG while at the same time it is feasible to increase efficiencies and heat rates. Improving the performance of the cycle means generating more electricity with fewer resources (economical, human and natural).

Motivation, purpose and scope

Several transformations are taking place in the electricity market and they are leading the world to a more efficient and more environmentally friendly course of action. This can only be achieved by modernizing the system. Renewable energies are slowly making progress, but these energies are not enough yet. The **motivation** of the combined cycle is to increase efficiency and output power while decreasing costs and environmental issues.

The **purpose** of this project is to develop a MATLAB® model which will reduce the total area of an HRSG, performing a thermodynamic analysis. This algorithm will have certain flexibility in order to be versatile for users with different objectives and requirements. Additionally, a multi pressure implementation and off-design calculations will be performed. From an academic point of view, this project will provide the author with a noteworthy knowledge regarding thermodynamics (specially heat transfer) and MATLAB® programming.

Regarding the **scope** of this project, it is significant to mention that this project is a thermodynamic analysis. It does not involve any thermo-economic or exergetic analysis. Furthermore, some elementary assumptions will be applied to the model. Those hypothesis are the following: steady state conditions (transient models are discussed elsewhere [2]), potential and kinetic energy changes are neglected, and evaporators do not take into account the biphasic state of the fluid. Other aspects of the HRSG such as mechanical stress, strain or structural integrity are not taken into consideration either.

1 Introduction

This section presents the current energy situation, so the reader can grasp the context of the model proposed. Additionally, some explanations are included about theoretical concepts, the software used and the regulations taken into account.

1.1 Current Energy Situation

The need for electricity is unquestionable in every aspect of our daily life. The electricity production has grown to a great extent during the last 30 years. As shown in Figure 1, the production went from 9866 TW h in 1985 to 28 416 TW h in 2016, duplicating its value in only 30 years. The tendency is clearly to continue to do so.

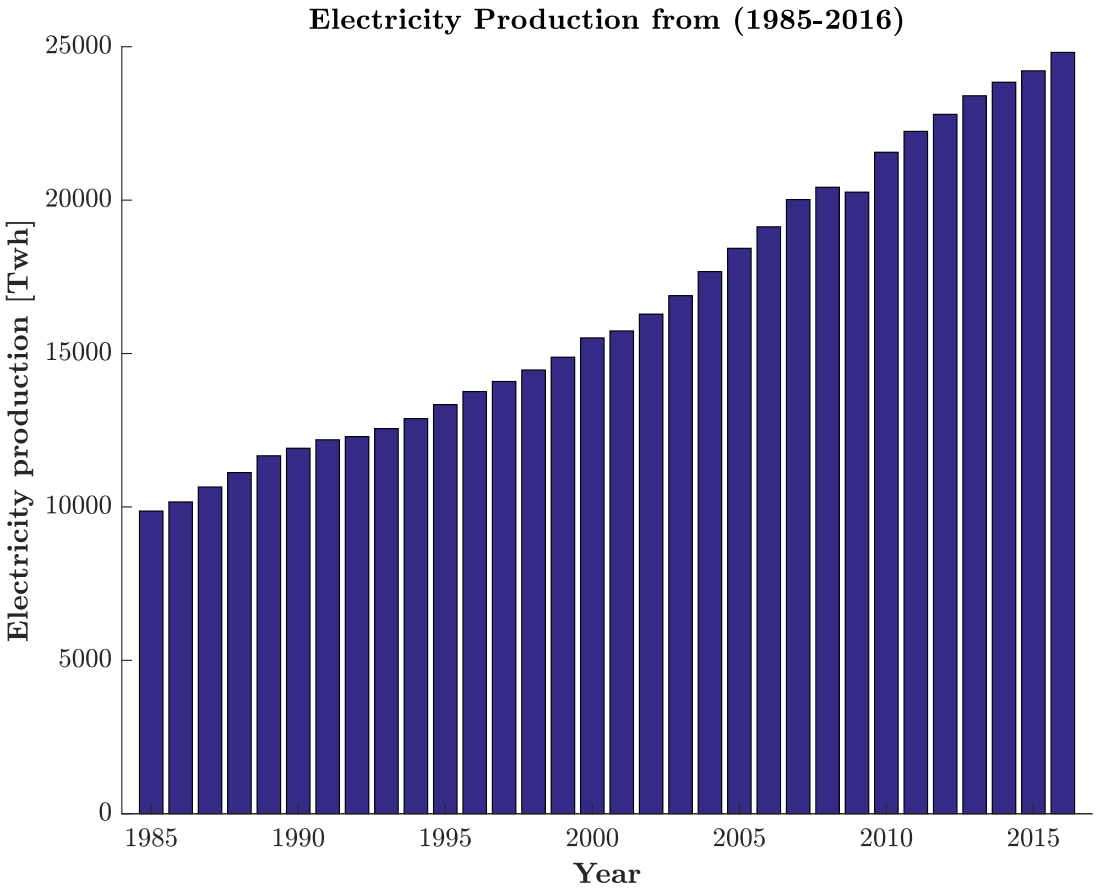

Figure 1: Electricity production (1985-2016) [1]

The ideal situation would be to produce a huge amount of electricity with a constant, cheap and environmentally friendly method, store it and then supply it as the market demands it. The problem is the difficulty to store electricity in large quantities [3]. Generation of electricity must meet the demand of the market in order to ensure the delivery to the power grid. The need of this resource is variable as well as unpredictable. There are algorithms based on historical data but you can never fully predict the demand with 100 % accuracy. Electricity production must be done according to the need of a particular moment in time.

Three main groups of primary energy sources are distinguished (Figure 2).

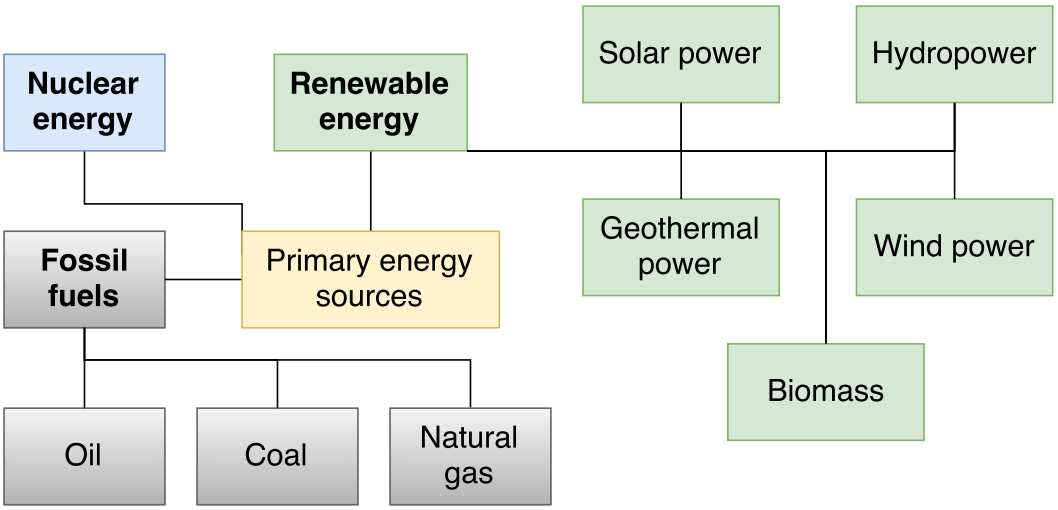

Figure 2: Primary energy sources

The booming of **renewable energy** is changing completely the market. One of the reasons is the increasingly awareness of the climate change effects, not only by the members of the energetic companies but also by the general population. Regulations are becoming more restrictive with the Kyoto Protocol [4], therefore technologies have to evolve to meet these new goals. Examples of renewable energies are hydropower, wind power, solar power and geothermal power. They still are a small portion of the primary energy consumption in the globe, only around 10 % [5]. However, they are growing at a very fast rate (up to 12 % from 2015 to 2016 [5]).

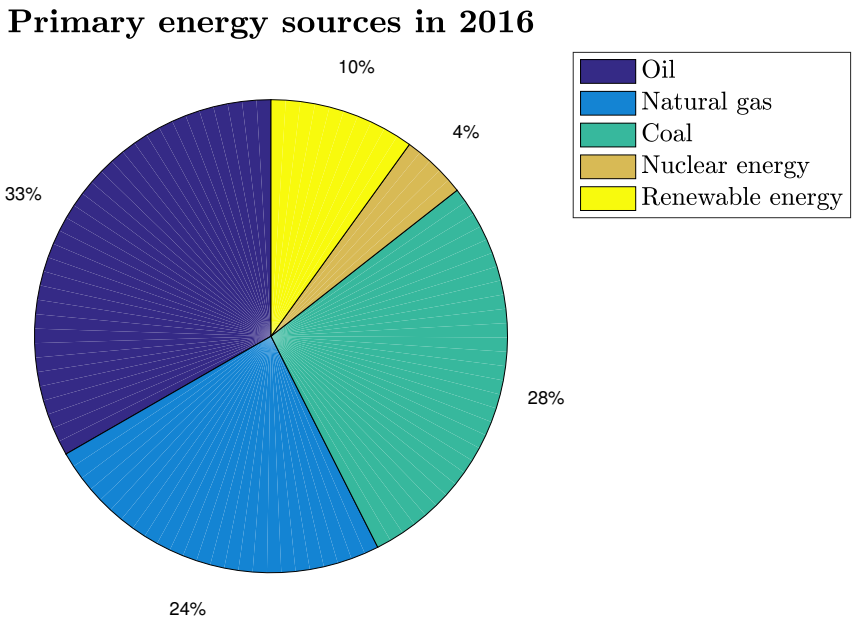

Figure 3: Primary energy sources percentages in 2016 [1]

The main advantages of these energies are the very little or non existent emission of pollutants, the low generation of waste and the vast quantity of resources available (such as sun rays, waves or geothermal heat). The major disadvantages are: the technology is still in stages of development, the impact on the fauna and flora (hydraulic dams or wind turbines) and a strong dependence of the climatology. In Spain there is great potential for renewable technologies due to the climatic conditions. In terms of annual production, in 2016 they accounted for the 40.8 % of the total electricity generation [6]. This way of obtaining energy is up to date neither constant nor predictable. For example, the contribution of the eolic energy ranges from a minimum rate of 3.1 % to a maximum of 52.1 % [6]. These numbers affirm the large variability that these technologies have. Therefore, we need technological solutions that allow us to produce energy in a reliable, flexible, low-emission and efficient way.

Nuclear energy accounted for 23.1 % of annual production in Spain during 2016 [6]. Energy is released when fissile isotopes like U-235 are bombarded with slow-moving neutrons. This process is called induced fission and it produces some decay heat (α, β and γ rays), around 2.4 fast-moving neutrons and a large amount of heat (approximately 193 MeV). One of the fast released neutrons is slowed down with a moderator like heavy water or graphite and the remaining neutrons are captured with control rods of boron. The slow-moving neutron collides with more U-235 producing a chain reaction which causes more fission events. The heat produced by this process is used in a steam Rankine cycle. The low CO_2 emissions [7] and the non-climate dependency (full availabilty 24 hours a day) make this technology a great investment for governments. However, it is still controversial mainly due to the operational safety and radioactive waste disposal [7]. Until these problems are solved, another definitive solution is needed.

Production of energy with **fossil resources** was the predominant source in 2016. As it was stated in Figure 2, non-renewable sources are coal, oil and natural gas. In Spain, they were up to 59.2 % of the total production [6]. Thermal power plants take advantage of the chemical energy of fossil fuels. The basic principle is to extract energy from a fluid by expanding it into a turbine. The shaft of the turbine is connected to an electric generator. The different configurations of power plants depend on the fuel burnt in the combustion and the fluid used for the cycle. There are two main types of cycles: gas and water, called Brayton and Rankine respectively.

The large amount of energy that the fossil fuels have for a relatively low cost is their main advantage. The emmision of pollutants is undoubtedly the critical disadvantage. The extraction of **oil** is not only used for electricity production, it is also the world's primary fuel transportation. Once it is extracted crude oil is processed to produce gasoline, pesticides, pharmaceutical and plastics [8]. **Coal** is widely used around the world because is quite abundant. It is proved to be one of the cheapest way to produce electricity, however, the main drawback is the large CO_2 emissions. **Natural gas** is the cleanest primary energy source [9]. It produces fewer undesirable products. Among those products, it produces about 1/2 of CO_2 and 1/10 of NO_x compared to oil and coal.

The leading purpose of this project is to model a thermal power plant that produces more power with less energy and less harmful pollutants. Combined cycle power plants provide an efficiency up to $\eta \simeq 60\,\%$. This technology has been used for more than 30 years, but the need for higher power outputs demand an increase in the efficiency. This type of power plants consist of a gas cycle (using natural gas as the working fluid) coupled with a steam cycle (using water as the working fluid). Some theoretical concepts need to be introduced in order to understand the approach of this project.

1.2 Theoretical Concepts

The idea of a combined cycle is fairly simple at the beginning. It is a combination of two cycles, a Brayton cycle followed up by a Rankine cycle. But before analyzing the combined cycle, it is necessary to mention other cycles.

1.2.1 Carnot Cycle

This cycle is defined as the maximum theoretical efficiency for a thermal cycle [10]. This cycle exchanges energy between a hot reservoir and a cold reservoir in order to obtain mechanical power. All the power cycles are based on this concept and their final goal is to achieve Carnot efficiency.

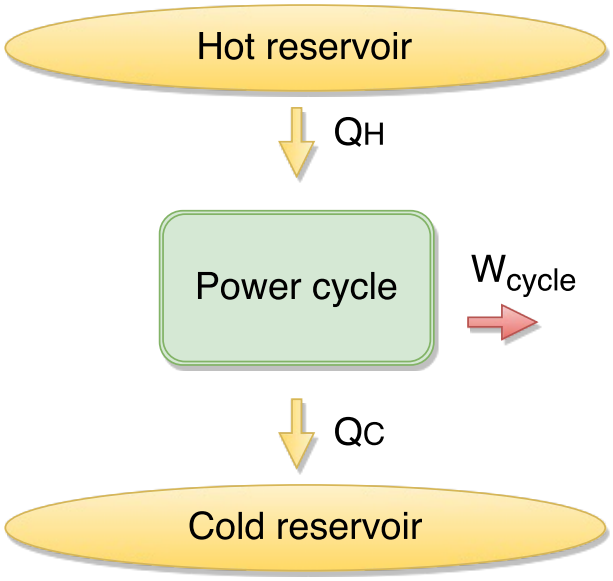

Figure 4: Power cycle

$$\eta_{Carnot} = \frac{W_{cycle}}{Q_{in}} = \frac{W_{cycle}}{Q_H} = 1 - \frac{Q_C}{Q_H} = 1 - \frac{T_C}{T_H} \tag{1}$$

In order to introduce the idea, a cycle that has 1400 K in the hot reservoir and 300 K in the cold reservoir would achieve a $\eta_{Carnot} \simeq 78.9\,\%$. This would only be in an ideal system without any thermal or mechanical loses. Real power cycles yield to an efficiency of $\eta \simeq 40\,\%$.

1.2.2 Brayton Cycle

The **Brayton Cycle** is a thermodynamic cycle that uses gas as working fluid. The gas is compressed to a high pressure, then it is mixed with fuel in the heat exchanger (or combustion chamber) to increase the temperature. The fluid is finally expanded in the turbine to generate electricity or propel vehicles [10]. The cycle can be open or closed as shown in Figure 5 and Figure 6. The closed one needs an extra heat exchanger to cool down the gas after the expansion (it uses natural gas, CO_2, Ne or Ar as the working fluid). The open cycle uses air and releases it to the atmosphere.

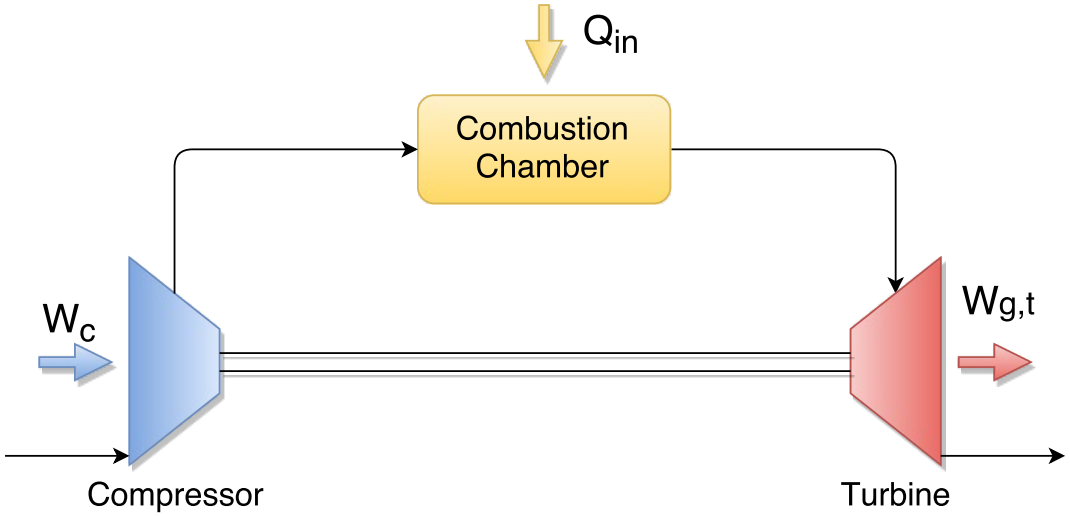

Figure 5: Open Brayton cycle

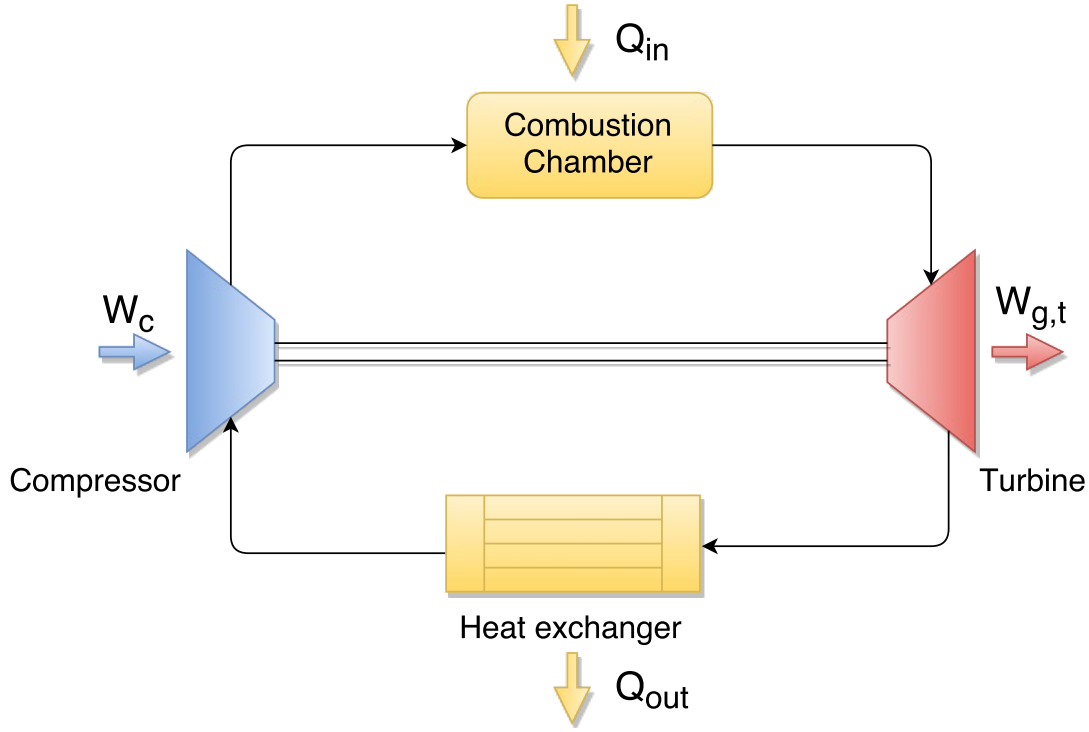

Figure 6: Closed Brayton cycle

Ideal thermal efficiency of this cycle is given in Equation 2.

$$\eta_{Brayton} = \frac{W_{cycle}}{Q_{in}} = 1 - \pi^{\frac{1-\gamma}{\gamma}} \tag{2}$$

Where π is the compression ratio of the cycle and γ is the specific gas ratio. As it is shown, the efficiency of the cycle strongly depends on π. There are many studies regarding this dependance [11]. However, it is not the scope of this project.

If $\pi = 15, \gamma = 1.4$ then $\eta_{Brayton} = 54\,\%$. This is an ideal value. If the isentropic efficiency of all the elements and other mechanical and thermal loses are taken into consideration, the real value is around $\eta_{Brayton} \simeq 25\,\%$. This value could be enhanced. That is why some alternatives are proposed [10]. The improved Brayton cycle includes reheating, cooling and regeneration. They can significantly increase the efficiency of the cycle. As shown in Figure 7, the configuration is not simple, but it yields to a higher efficiency: $\eta_{Brayton} \simeq 35\,\%$.

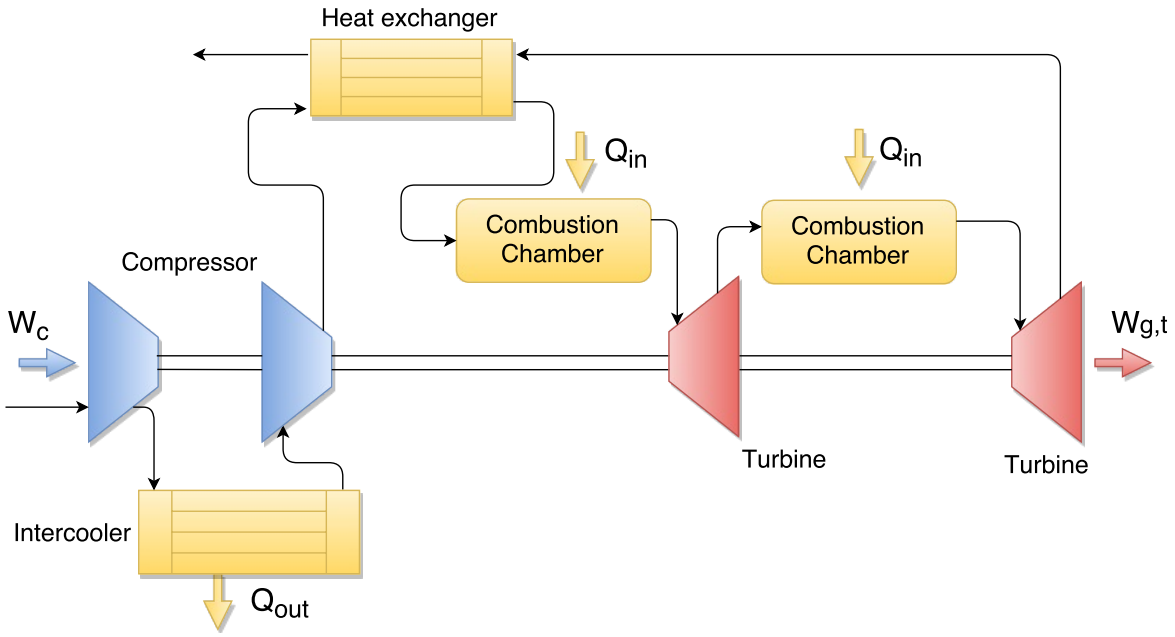

Figure 7: Improved Brayton cycle

1.2.3 Rankine Cycle

The **Rankine Cycle** is a thermodynamic cycle that uses water as the working fluid. It is important to remark that the fuel and cycle fluid are never in contact; therefore, several types of fuel can be used such as coal or oil among others. The heat of the fuel is transferred to the water that is previously compressed in the boiler. The fluid expands in the turbine and it makes the electricity generator move. This cycle usually has an efficiency of $\eta_{Rankine} = 30\,\%$. Figure 8 shows the schematic diagram of the cycle.

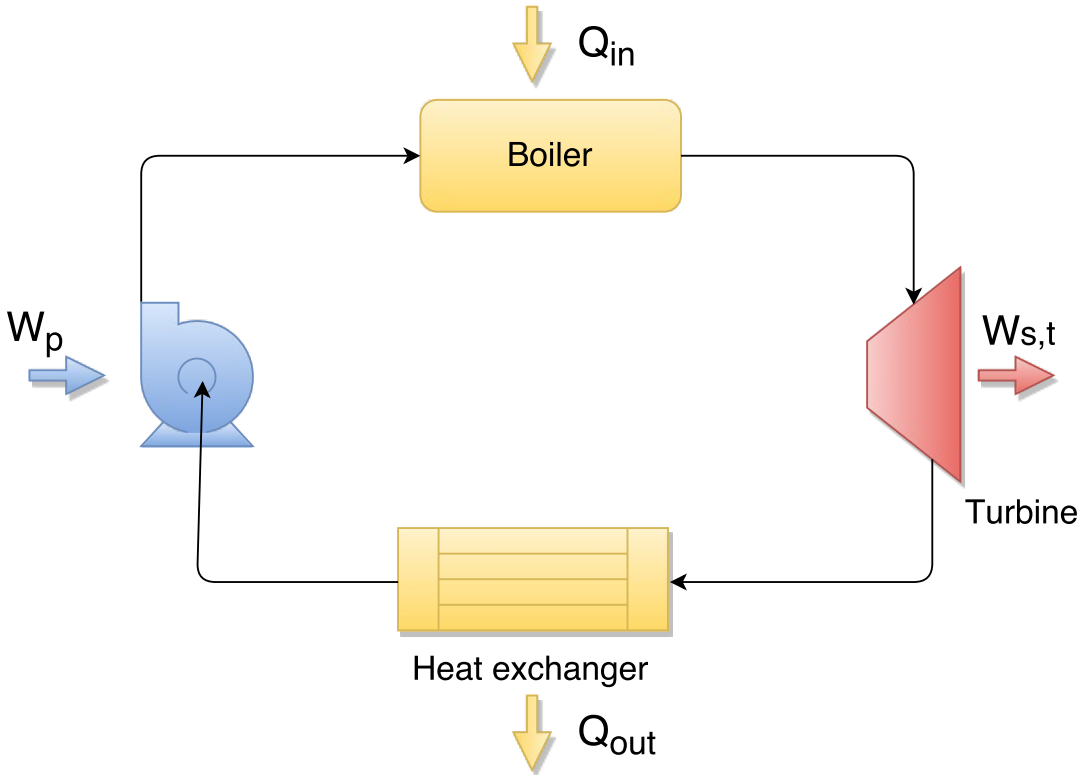

Figure 8: Rankine cycle

Thermal efficiency of this cycle is given in Equation 3.

$$\eta_{Rankine} = \frac{W_{cycle}}{Q_{in}} = 1 - \frac{Q_{out}}{Q_{in}} \tag{3}$$

In the same way as the Brayton cycle, Rankine cycle can be improved. Reheating, regeneration (open or closed feedwater heaters) can be implemented as shown in Figure 9. This improved Rankine cycle can achieve efficiencies such as $\eta_{Rankine} = 40\,\%$.

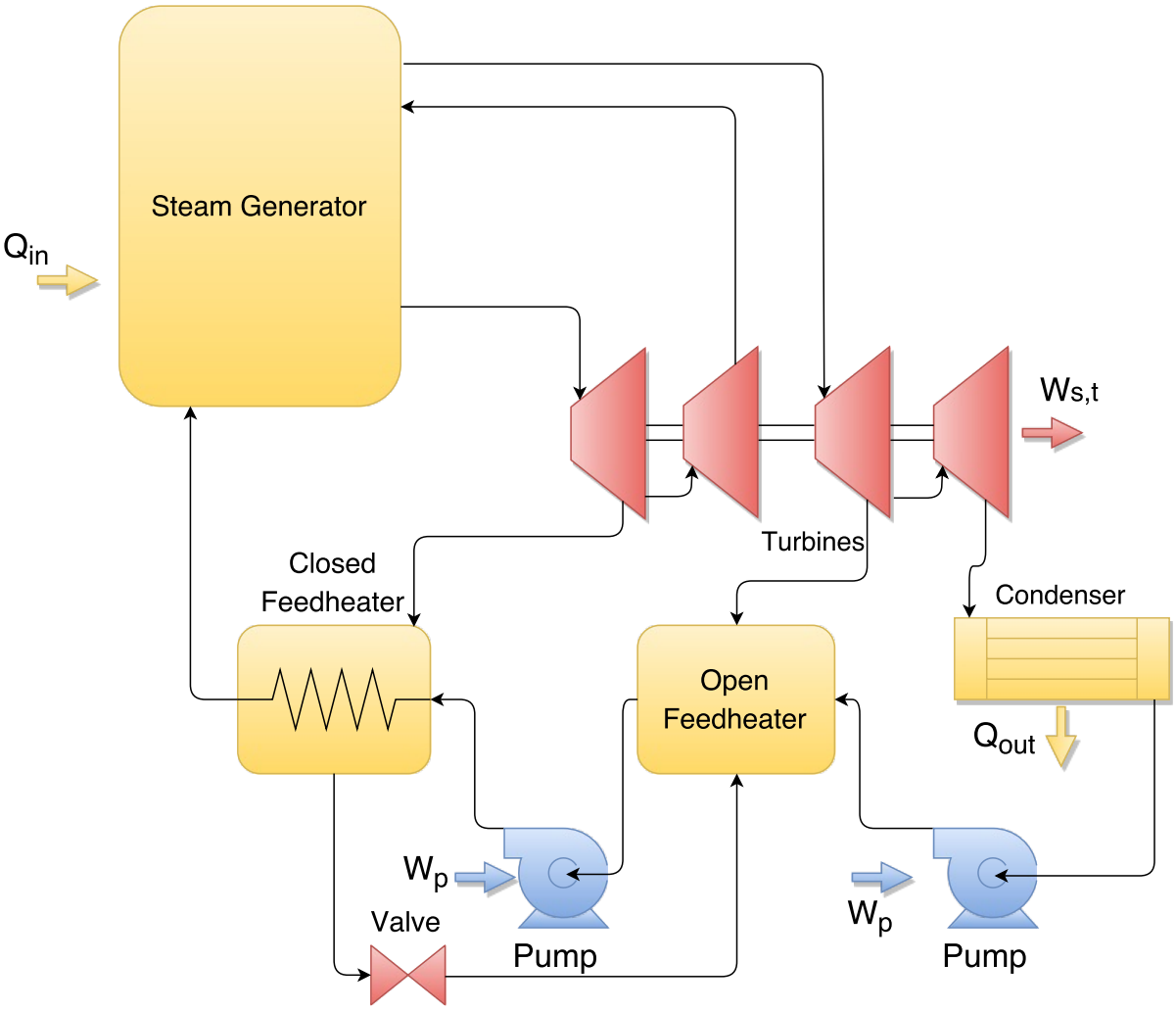

Figure 9: Improved Rankine cycle

1.2.4 Combined Cycle

Combined cycle power plants (CCPP) connect a Brayton cycle with a Rankine cycle. The idea is to deliver the high energy of the exhaust gases of the Brayton cycle (that otherwise would have been lost in the Brayton cycle alone) to a steam flow. This considerably increases the efficiency of the cycle and the power output because the electricity produced in the steam turbine needs no fuel at all. The element that connects both cycles is the heat recovery steam generator (HRSG). The performance of the whole system strongly depends on the optimal integration of the power units [12], therefore, the HRSG is the most critical component of the cycle. The modeling and optimization of the HRSG is the main purpose of this project.

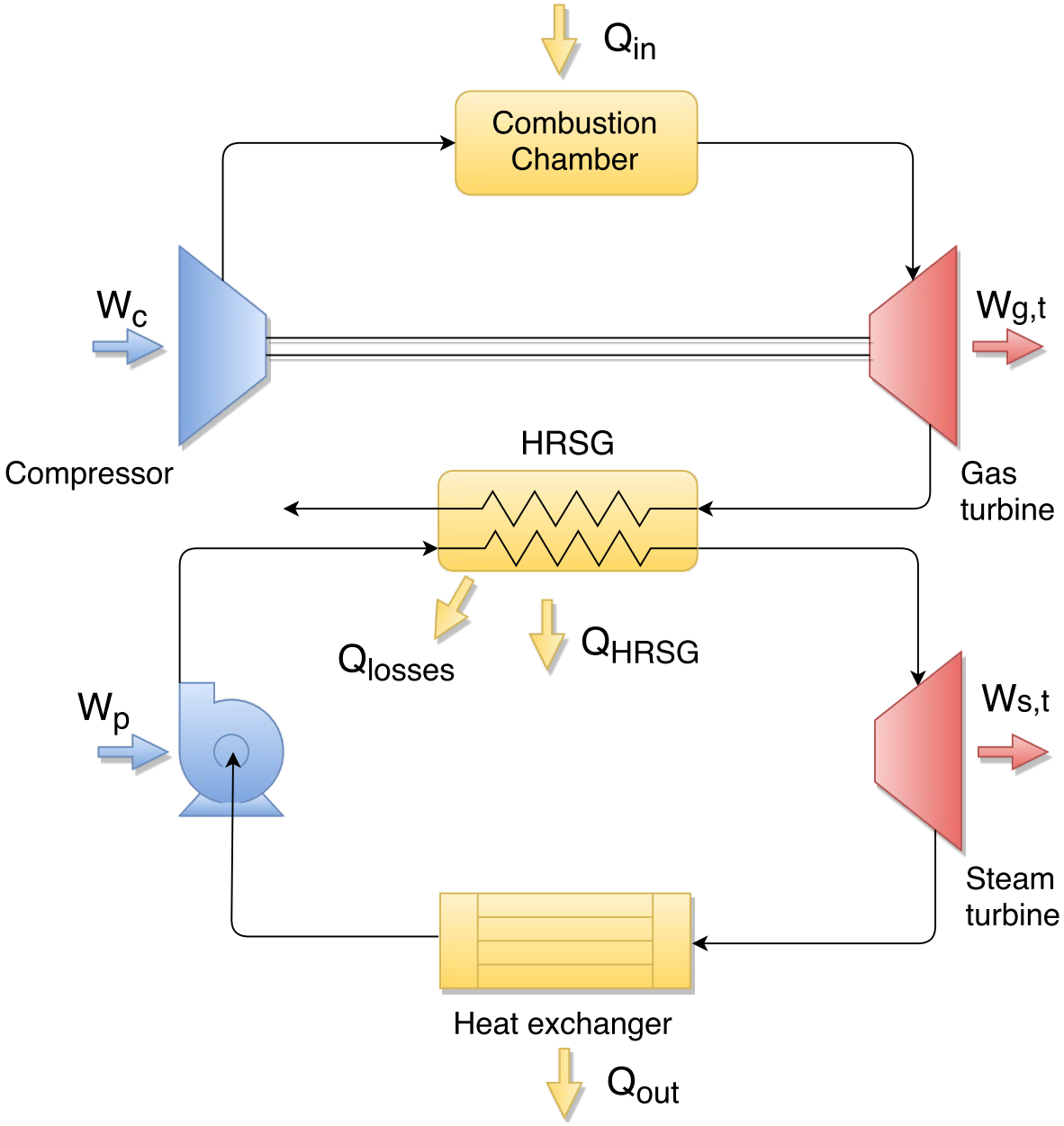

Figure 10: Combined cycle

Ideal thermal efficiency for this cycle is obtained in Equation 4.

$$\eta_{Brayton} = \frac{W_{g,t}}{Q_{in}} \quad \text{and} \quad \eta_{Rankine} = \frac{W_{s,t}}{Q_{HRSG}}$$

$$\eta_{CC} = \frac{W_{cycle}}{Q_{in}} = \frac{W_{g,t} + W_{s,t}}{Q_{in}} = \eta_{Brayton} + \eta_{Rankine} \cdot \frac{Q_{HRSG}}{Q_{in}} \tag{4}$$
$$\eta_{CC} = \eta_{Brayton} + \eta_{Rankine} \cdot (1 - \eta_{Brayton})$$

For example, if $\eta_{Brayton} = 35\,\%$ and $\eta_{Rankine} = 44\,\%$, then $\eta_{CC} = 63.6\,\%$.

CCPP comprise numerous **advantages** in power generation. Higher efficiency than both gas and steam cycles (up to $\eta_{CC} = 60\,\%$), low CO_2 and NO_x emissions (natural gas is usual the fuel used in the Brayton cycle), short construction time, low investment cost and low operational and maintenance costs [13]. Other authors mention the fast start-up capabilities or the lower cooling water requirements [14]. The main **disadvantages** are the strong dependency from the gas cycle (Rankine cycle would not work without the first cycle) and the emission of pollutants (in comparison to the renewable technologies).

The **HRSG** is a heat recovery steam generator that transfers the energy from the gas to the steam. It can be designed with different configurations based on: once-through, natural or forced circulation, unfired or fired, single or multi pressure, water or fire tubes, integral or elevated drum, in-line or stagerred arrangements, horizontal or vertical, etc. This is throughly discussed in [15]. At the end, a water tube (due to the clean gases), fired (more flexibility of the CCPP and controlled temperatures in the steam cycle), staggered, forced circulation (horizontal steam flow and vertical gas flow) and multi pressure with reheat (increases efficiency) HRSG is recommended. A model of a multi pressure combined cycle is described later in section 2. The elements of a single pressure HRSG are shown in Figure 11.

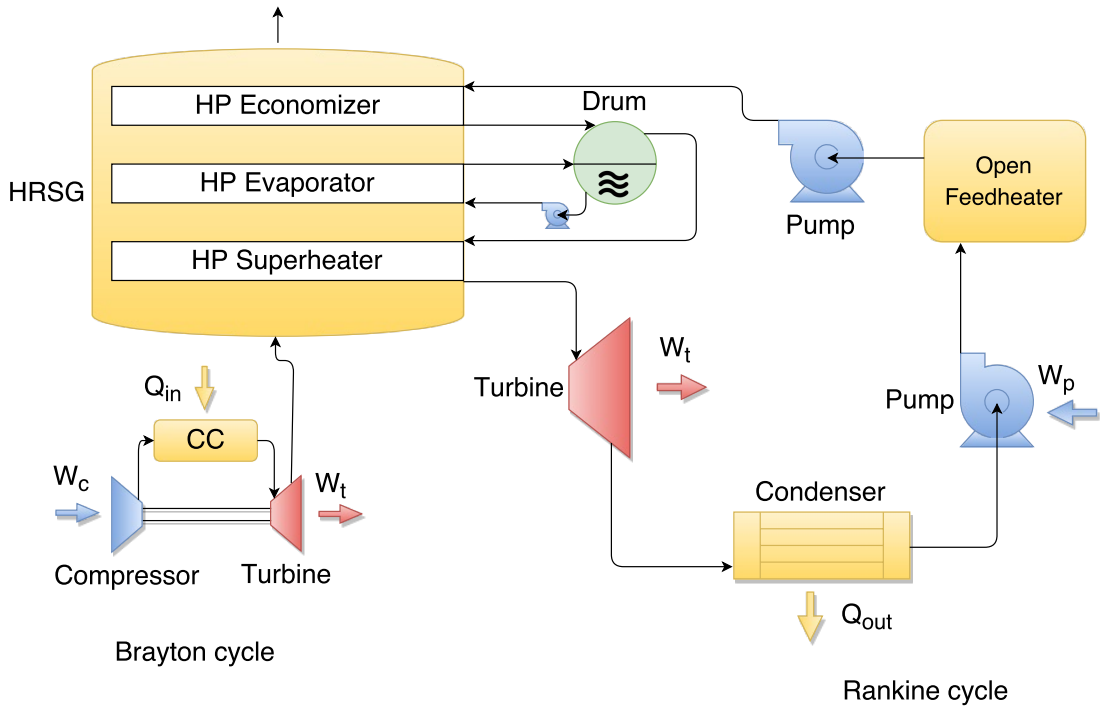

Figure 11: HRSG elements

Geometric properties of the HRSG are given in Figure 12.

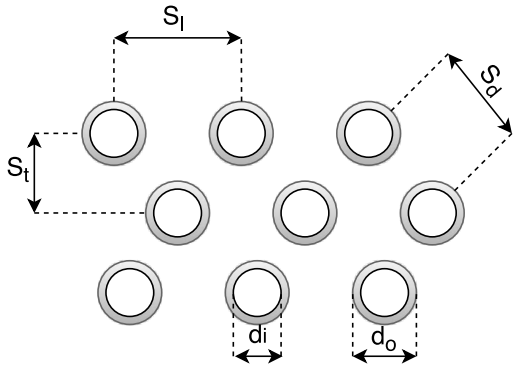

Figure 12: HRSG geometric variables

The gas flows from the bottom part to the top one. It gradually decreases its temperature due to the heat transfer to the vapor system. The exhaust gases exit the HRSG at an approximate temperature of 100 °C. The water flows inside tubes in a opposite direction (counter flow circulation maximizes the heat transfer). The trajectory of the steam is economizer, drum, evaporator, drum (again) and superheater. After this process the superheated steam flows to the steam turbine to generate electricity. The purpose of each element is described below:

- *Economizer:* The liquid water that comes from the condenser is heated in the economizer close to saturation state. Temperature approach point (AP) is the difference between the outlet of the economizer and the saturation temperature. This value ranges from 5 °C to 25 °C according to various sources [16] [17].

- *Drum:* The drum is a key element in the system due to its main functions. First, it absorbs the transient states when the plant starts up or stops. Second, it separates the steam from the liquid by centrifugal processes. And last, it regulates temperature and pressure. Liquid water enters the drum and then, saturated liquid water exits to the evaporator with a circulating pump.

- *Evaporator:* Steam is obtained with the change of phase of the liquid. This process is done approximately at constant pressure. The steam enters the drum again after the evaporator. Temperature difference between the saturation temperature and the gas temperature is called pinch point (PP), it is usually between 5 °C and 20 °C [18]. This parameter greatly affects the performance of the HRSG as it will be explained in section 2.

- *Superheater:* After the evaporator, steam enters the drum and it mixes with the biphasic fluid. Saturated steam is extracted from the top part of the drum and it is directed to the superheater. This is where superheated steam is produced. Most of the heat transfer is done in this element to the high temperatures of the gas. After the superheater, the flow goes to the steam turbine.

Temperature profiles are extensively used in this project. Figure 13 shows temperatures of the gas side and water side against heat transferred. It can be seen how the gas temperature decreases as the energy is transferred to the steam side of the HRSG. The area in between the gas and steam line flow represent the heat losses that take place in the HRSG.

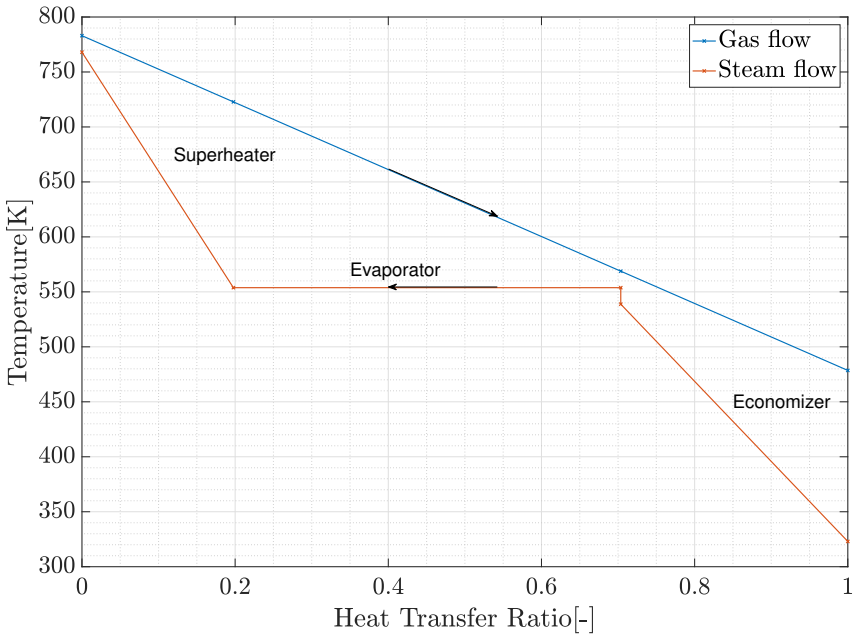

Figure 13: HRSG temperature profile

Taking into account those heat losses in the cycle, the effectiveness of a heat exchanger (HRSG), ε_{HRSG}, is defined in Equation 5. Then, the total efficiency of the cycle can be recalculated as presented in [19].

$$\begin{aligned} \varepsilon_{HRSG} &= \frac{Q}{Q_{max}} = \frac{Q_{HRSG}}{Q_{HRSG} + Q_{losses}} = \frac{Q_{in}}{Q_{HRSG} + Q_{losses}} \cdot \frac{Q_{HRSG}}{Q_{in}} \\ \varepsilon_{HRSG} &= \frac{1}{1 - \eta_{Brayton}} \cdot \frac{Q_{HRSG}}{Q_{in}} \\ \eta_{CC} &= \eta_{Brayton} + \varepsilon_{HRSG} \cdot \eta_{Rankine} \cdot (1 - \eta_{Brayton}) \end{aligned} \tag{5}$$

For example, if $\eta_{Brayton} = 35\,\%$, $\eta_{Rankine} = 44\,\%$ and $\varepsilon_{HRSG} = 83\,\%$, then $\eta_{CC} = 58.7\,\%$.

1.2.5 State of the Art

Overall efficiency of the CCPP can be enhanced with several methods. The latest improvements have been conducted regarding HRSG parameter optimization and gas turbine cooling techniques.

- Regarding the **HRSG**, three pressure levels with reheat is the most common configuration due to the high efficiency of the CC, close to $\eta_{CC} = 60\,\%$. More improvements in the overall efficiency can be achieved with reduction of irreversibilities in the HRSG [20], performing exergy analysis [21] or thermoeconomic analysis [22]. Other methods will be later discussed in subsection 2.3 since optimization of the HRSG is the main purpose.
- Concerning **gas turbines**, higher combustor outlet temperature (COT) means more power output, therefore, greater overall efficiency. At this moment, the efficiency is limited by the thermal properties of the turbines components. Cooling blade technology allows the increase of this value without compromising the integrity of the materials. Most turbine manufacturers set their COT to 1500 °C [23]. Recent studies show that COT of 1700 °C can be achieved [24]. Along with the cooling improvements, Kotowicz shows that high pressure ratios can increase the overall efficiency up to $\eta_{CC} = 64\,\%$ [23].

1.3 Software

- *MATLAB®*: This software was used with the **uc3m** student license. The mathematical model, optimization, figures and graphs were made with this program.
- *LaTeX*: This text editor broaden the possibilities of customization of this project. Items such as the cover, list of contents, chapters, table of figures, captions and citations, cross-referencing were made possible with the free software license.
- *Coolprop*: Library that implements the properties of a fluid based on the Helmholtz energy formulation [25]. Any property of a wide variety of fluids can be obtained with two given properties.

1.4 Regulations

The regulations that apply to a CCPP are numerous, however, only environmental issues will be address in this section. Design of the power plant takes into account emissions from the start, therefore they have a big impact in the engineering project. In the case of a combined cycle plant, natural gas is the main fuel used. The main products of the combustion are N_2, O_2, H_2O, NO_x, CO_2, CO, UHC and SO_x [26]. All of them are toxic to the atmosphere and more importantly, to humans except for N_2, O_2 and H_2O.

- N_2, O_2 and H_2O are not dangerous gases. The atmosphere air mixture already contains them, therefore they are harmless for the population.
- NO_x emissions strongly increase with firing temperature and fuel-to-air ratio [26]. Emissions can be reduced cooling the flame with injection water techniques in the turbine [27].
- CO_2 emissions are significantly lower when using natural gas compared to conventional coal plants. It is the main responsible for the global warming effect.
- CO is product of an incomplete combustion in the turbine. It is very dangerous because it is odorless and colorless.
- UHC are unburned hydrocarbons, they form because of the incomplete oxidation of the fuel.
- SO_x can cause acid rain. They can be reduced by limiting the sulfur content of the fuel [26].

The maximum emissions of these gases that a power plant can produce are limited by local regulations.

2 Calculations

A detailed procedure for all the calculations of the project is presented in this section. Four main calculations are performed in the project: single pressure model, optimization of single pressure model, multi pressure model and off-design calculations.

2.1 Definition of the problem

Figure 14 and Figure 15 show the details of a multi pressure model. A three pressure HRSG significantly increases the efficiency of the cycle because of the better use of the energy. The heat transfer is carried out in a more productive way because the temperature differences between the temperatures of gas and the steam are smaller. The details of the model are described below. Reference points (e.g., $T3_s$) are shown in both figures, they will be used later on in subsection 2.2.

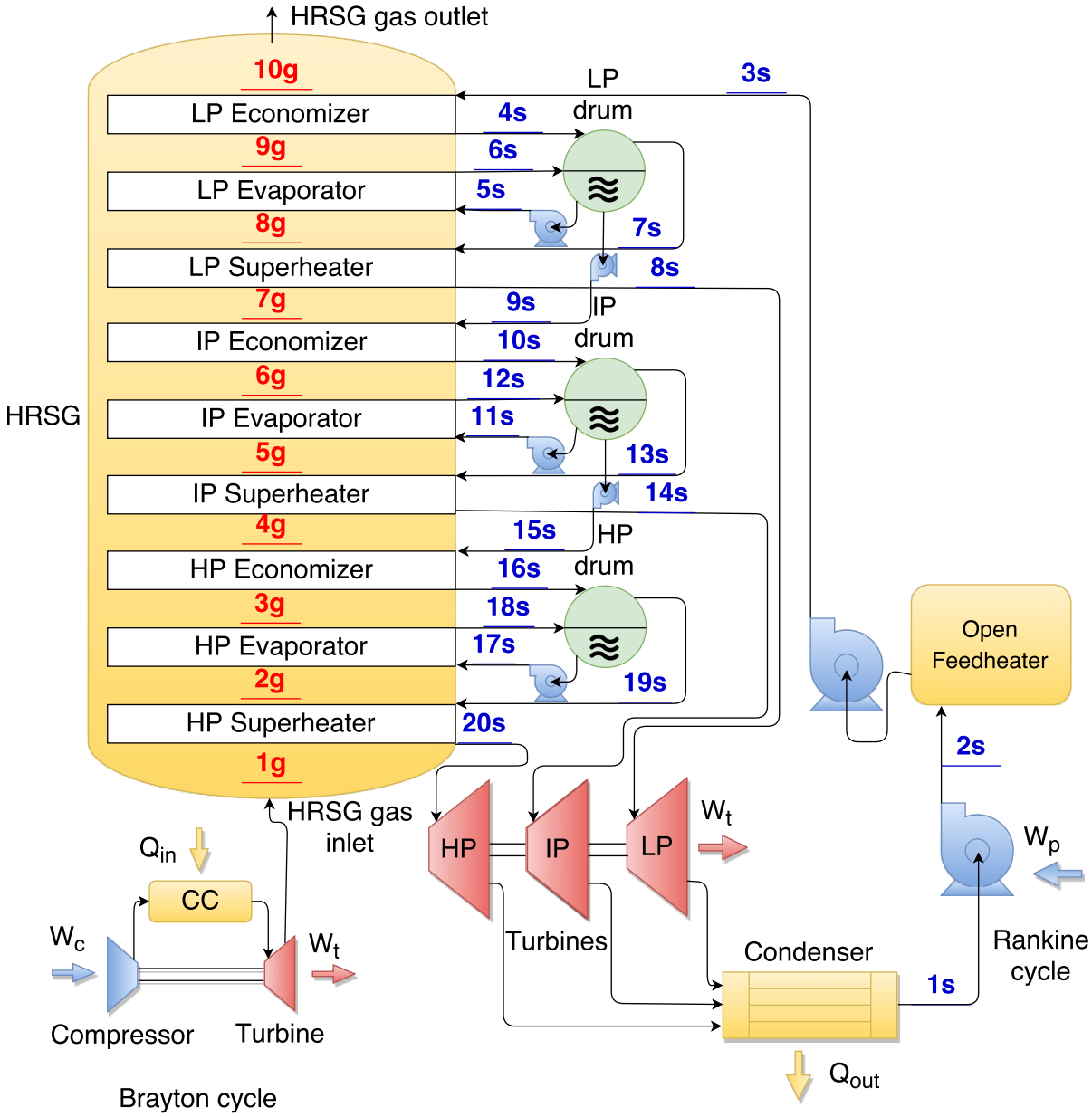

Figure 14: Multi pressure CC diagram

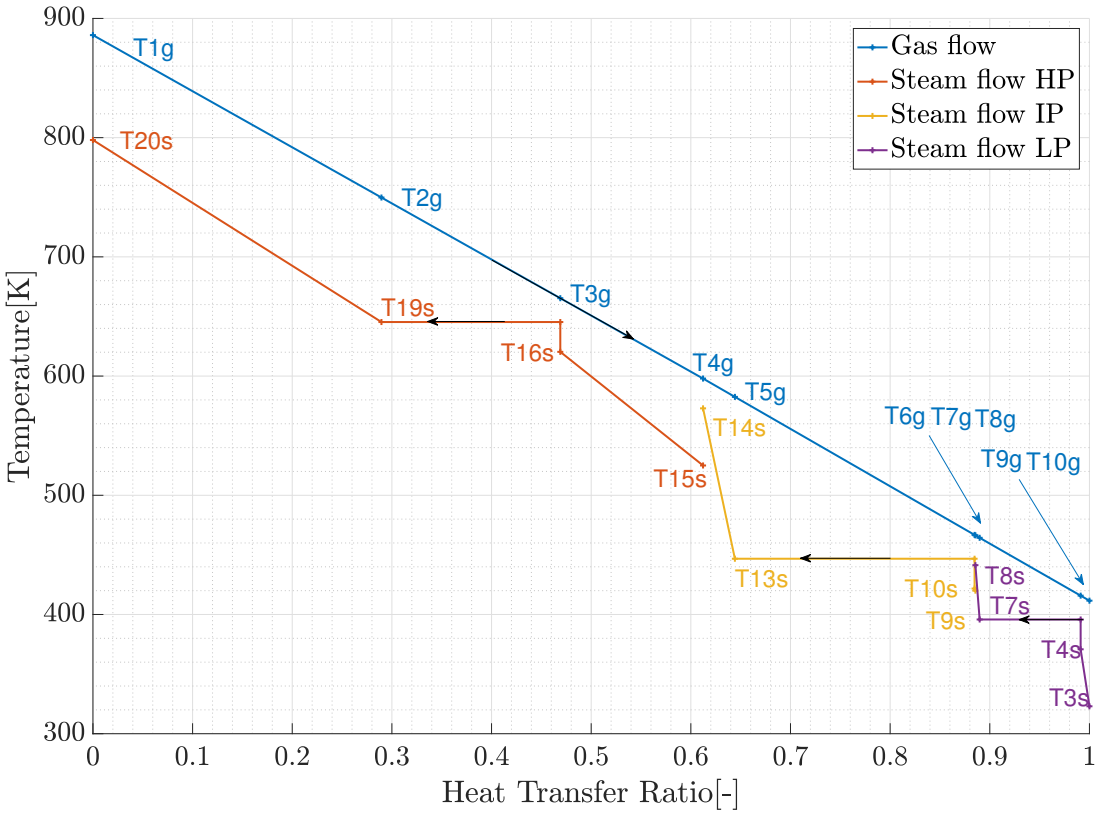

Figure 15: Multi pressure CC temperature profile

As it was enunciated before, the energy of the exhaust gases is transferred to the water in various stages. The multi pressure schematic is based on the single pressure one, only adding two more pressure levels. This implies the incorporation of three different economizers (EC), evaporators (EV), superheaters (SH), drums, turbine units and circulating pumps. The low pressure level (LP) is the one that lasts encounters the gas, that is why it is located at the top of the HRSG (vertical configuration was the one selected). The water comes from the feedheater and it goes through the $EC\ LP$, $EV\ LP$ and $SH\ LP$. After this stage, the superheated steam goes directly to the LP steam turbine unit. The remaining water in saturated liquid stage from the low pressure drum is pumped into the intermediate pressure level (IP). It goes through the IP elements and it is finally expanded in the IP steam turbine. The high pressure level (HP) mirrors the procedure of the other pressure levels. It is important to remark the mass vapor quality of some fundamentals points of the cycle. The state of the fluid that enters the evaporator is in liquid saturated state and the vapor that enters the superheater is in vapor saturated state. At last, the liquid that exits the drum to the next pressure level is in liquid saturated state.

As it is shown in 1.2.4, there are numerous factors and properties that define a HRSG. However, it is not clear to what extent some of those parameters affect the performance of the HRSG or the entire CCPP. When the calculations are done by hand, it could take ages to figure out what the most important variables are. It could be the exit temperature of the gas turbine, the approach temperature or the number of columns of the HRSG. On the other side, distinguished power plant companies buy commercial software programs (such as Thermoflow or Gatecycle) that do all these calculations for you, but they are not affordable (not even for some energy companies). Another approach is to look into the latest scientific articles. However, they present their results based on their requirements, which are not always the ones you have. The solution for this problem relies on a flexible MATLAB® model that is developed based on the fundamental equations of heat transfer.

- Proposed solution

The solution that is proposed is a versatile model in which you enter specific input data (requirements of the engineering project) and based on this information, it calculates the rest of the parameters of the HRSG. Additionally, this program optimizes these parameters to obtain the best output possible for the power plant. This model takes into account most aspects of the real life problem. Calculations of the temperature, pressure, heat transfer, inside and outside coefficients, global heat transfer coefficient and area for every element of the HRSG (economizer, drum, evaporator and superheater) for all the pressure levels (LP, IP, HP) are made with this model. Furthermore, considering the change of the properties with the change of temperature and pressure gives an added value to the project. Moreover, validations of this model with real data must be carried out later in order to authenticate the method.

2.2 Mathematical model description

The following description of the model is a mathematical approach based on the heat transfer equations for heat exchangers found in [19]. This equation is based on the assumptions that Q is the total heat rate transfer between the hot and cold fluid, neglecting heat transfer to the surrounding and kinetic and potential energy changes. The main goal of the model is to calculate all the parameters of the HRSG.

$$Q = U \cdot A \cdot F \cdot \Delta T_{lm} \tag{6}$$

Equation 6 defines the basic equation of a heat exchanger. The aim of the calculation is to obtain the area of heat transfer (A). Therefore, the rest of the parameters must be calculated first. The single pressure model will be explained and then it will be extended for a multi pressure model. The schematic diagram is shown in Figure 16.

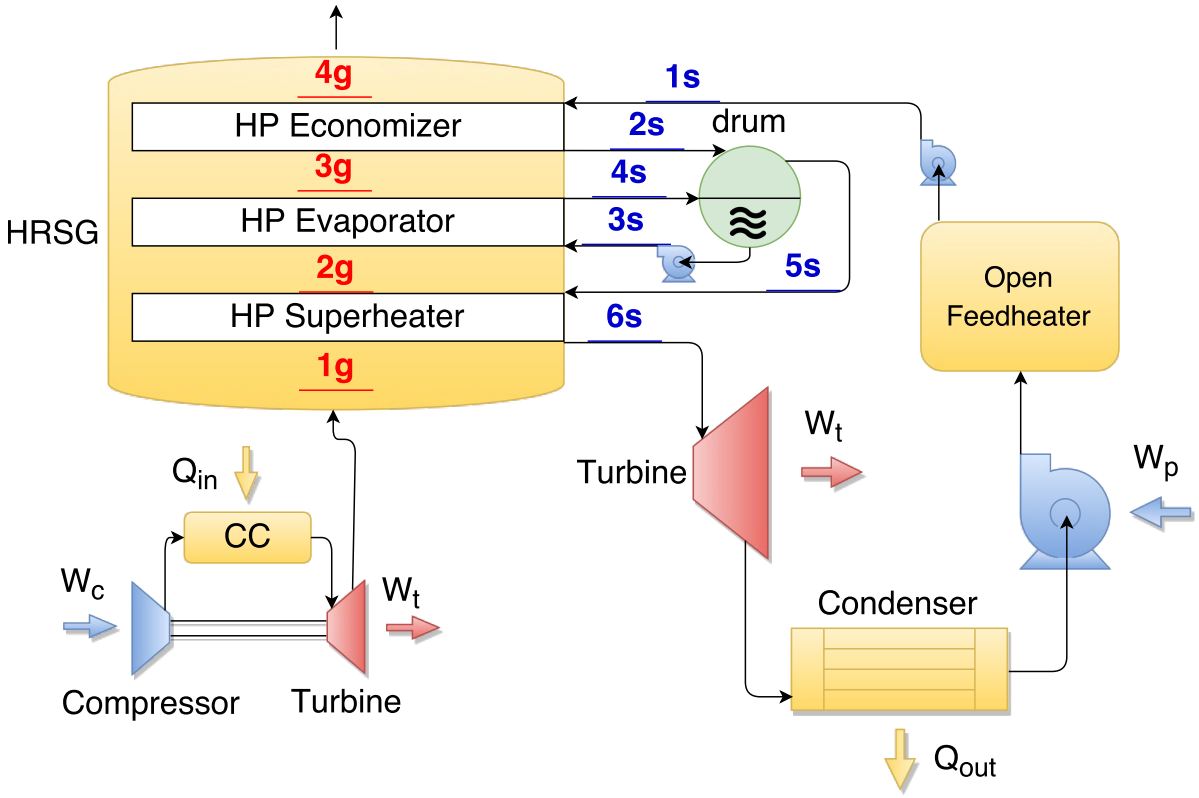

Figure 16: Single pressure CC diagram

The procedure of the calculations employed in this project is the following and it is explained in the next sections.

Input data (2.2.1)

↓

Properties of steam and gas (2.2.2)

↓

Heat transfer rate (2.2.3)

↓

UA value(2.2.4)

↓

Gas heat transfer coefficient (2.2.5)

↓

Steam heat transfer coefficient (2.2.6)

↓

Global heat transfer coefficient (2.2.7)

↓

Area (2.2.8)

↓

Efficiency (2.2.9)

↓

Multi pressure (2.2.10)

2.2.1 Input data

The following input data is used in the model. The values for these parameters have been exhaustively investigated to get the most common values from the latest scientific articles. Other values are assumptions made for this problem. The pressure drop in the evaporator is negligible, therefore $PD_{s,EV} = 0$. Due to the characteristics of the drum (explained in 1.2.4) $X5_s = 1$. The number of rows and columns is known to be between 4 and 12 according to [28].

Description	Parameter	Value	Unit	Reference
HRSG properties	AP	15	K	[29]
	PP	15	K	[29]
Gas properties	M_g	650	kg/s	[30]
	$T1_g$	783	K	[31]
	$P1_g$	1.013	bar	[31]
Steam properties	$T1_s$	323	K	[31]
	$T6_s$	768	K	[31]
	$P6_s$	60	bar	[31]
	$PD_{s,SH}$	8	%	[32]
	$PD_{s,EV}$	0	%	–
	$PD_{s,EC}$	25	%	[32]
	$X5_s$	1	–	–
Geometric properties	L_t	15.3	m	[30]
	d_o	53	mm	[31]
	d_i	50	mm	[31]
	S_t	66	mm	[33]
	S_l	66	mm	[33]
	$N_{c,SH}$	10	–	[28]
	$N_{c,EV}$	10	–	[28]
	$N_{c,EC}$	10	–	[28]
	$N_{r,SH}$	10	–	[28]
	$N_{r,EV}$	10	–	[28]
	$N_{r,EC}$	10	–	[28]
CC properties	$\eta_{Brayton}$	35	%	-
	$\eta_{Rankine}$	44	%	-

Table 2: Single pressure input data

2.2.2 Properties

Coolprop is the ideal tool for this model because it can be implemented in the MATLAB® code. Most of the properties of the fluids are included in the libraries such as specific enthalpy, temperature, pressure, density, etc. Two independent thermodynamic properties are needed in order to calculate the rest of them as it is shown in Equation 7.

$$\left.\begin{array}{r} T = 500\,\mathrm{K} \\ P = 100\,\mathrm{bar} \\ Water \end{array}\right\} \xrightarrow{\text{Coolprop}} H = 977\,\mathrm{kJ/kg} \tag{7}$$

Energy balance equations are the base of this model. The properties of the reference points will be calculated in order to perform the heat transfer calculations taking into consideration the data from Table 2. For the steam side, the following calculations are carried out:

$$
\begin{aligned}
&\left.\begin{matrix} T6_s \\ P6_s \\ Water \end{matrix}\right\} \xrightarrow{\text{Coolprop}} H6_s \\
&P5_s = P6_s \cdot (1 + PD_{s,SH}) \\
&\left.\begin{matrix} X5_s \\ P5_s \\ Water \end{matrix}\right\} \xrightarrow{\text{Coolprop}} \begin{matrix} H5_s \\ T5_s \end{matrix} \\
&T3_s = T5_s \\
&\left.\begin{matrix} T3_s \\ X3_s \\ Water \end{matrix}\right\} \xrightarrow{\text{Coolprop}} \begin{matrix} H3_s \\ P3_s \end{matrix} \\
&T2_s = T3_s - AP_{HP} \\
&P2_s = P3_s \\
&\left.\begin{matrix} T2_s \\ P2_s \\ Water \end{matrix}\right\} \xrightarrow{\text{Coolprop}} H2_s \\
&P1_s = P2_s \cdot (1 + PD_{s,EC}) \\
&\left.\begin{matrix} T1_s \\ P1_s \\ Water \end{matrix}\right\} \xrightarrow{\text{Coolprop}} \begin{matrix} H1_s \\ T1_s \end{matrix}
\end{aligned}
\tag{8}
$$

The gas side calculations are based on the gas properties at the exhaust of the gas cycle. The air temperature and pressure are defined by the Brayton cycle.

$$
\begin{aligned}
&\left.\begin{matrix} T1_g \\ P1_g \\ Air \end{matrix}\right\} \xrightarrow{\text{Coolprop}} Cp_g \\
&T3_g = T3_s + PP_{HP}
\end{aligned}
\tag{9}
$$

2.2.3 Heat transfer

First, an energy balance equation across the SH and EV is done to obtain the steam mass flow, M_s.

$$Q_{SH-EV} = M_g \cdot Cp_g \cdot (T1_g - T3_g) = M_s \cdot (H6_s - H2_s) \tag{10}$$

$$M_s = \frac{M_g \cdot Cp_g \cdot (T1_g - T3_g)}{H6_s - H2_s} \tag{11}$$

Energy balance in the superheater to obtain temperature $T2_g$.

$$Q_{SH} = M_g \cdot Cp_g \cdot (T1_g - T2_g) = M_s \cdot (H6_s - H5_s) \tag{12}$$

$$T2_g = T1_g - \frac{M_s \cdot (H6_s - H5_s)}{M_g \cdot Cp_g} \tag{13}$$

Energy balance in the economizer to obtain temperature $T4_g$.

$$Q_{EC} = M_g \cdot Cp_g \cdot (T3_g - T4_g) = M_s \cdot (H2_s - H1_s) \tag{14}$$

$$T4_g = T3_g - \frac{M_s \cdot (H2_s - H1_s)}{M_g \cdot Cp_g} \tag{15}$$

Then, the heat transfer for every element of the HRSG can be calculated as:

$$\begin{aligned} Q_{SH} &= M_g \cdot Cp_g \cdot (T1_g - T2_g) \\ Q_{EV} &= M_g \cdot Cp_g \cdot (T2_g - T3_g) \\ Q_{EC} &= M_g \cdot Cp_g \cdot (T3_g - T4_g) \\ Q &= Q_{SH} + Q_{EV} + Q_{EC} \end{aligned} \tag{16}$$

2.2.4 UA value

From Equation 6, UA value can be specified for all elements of the HRSG where x stands for SH, EV or EC in Equation 17. The *log mean temperature difference* is obtained from a heat exchanger energy balance analysis [19], this value is used because local temperature difference changes with the HRSG position.

$$Q_x = UA_x \cdot F_x \cdot \Delta T_{lm,x} \tag{17}$$

Investigations about F_x (correction factor for ΔT_{lm}) have been performed elsewhere [34]. Conclusions are that HRSG's tubes (usually in a serpentine shape) behave as if they were in a pure counter flow heat exchanger. This implies that F_x is very close to unity, therefore the following assumption is used:

$$F_{SH} = F_{EV} = F_{EC} = 1 \tag{18}$$

Then, the UA values can be obtained.

$$\begin{aligned} \Delta T_{lm,SH} &= \frac{T1_g - T6_s - T2_g + T5_s}{Ln\left(\frac{T1_g - T6_s}{T2_g - T5_s}\right)} \\ UA_{SH} &= \frac{Q_{SH}}{F_{SH} \cdot \Delta T_{lm,SH}} \end{aligned} \tag{19}$$

$$\begin{aligned} \Delta T_{lm,EV} &= \frac{T2_g - T5_s - T3_g + T3_s}{Ln\left(\frac{T2_g - T5_s}{T3_g - T3_s}\right)} \\ UA_{EV} &= \frac{Q_{EV}}{F_{EV} \cdot \Delta T_{lm,EV}} \end{aligned} \tag{20}$$

$$\begin{aligned} \Delta T_{lm,EC} &= \frac{T3_g - T3_s - T4_g + T3_s}{Ln\left(\frac{T3_g - T3_s}{T4_g - T3_s}\right)} \\ UA_{EC} &= \frac{Q_{EC}}{F_{EC} \cdot \Delta T_{lm,EC}} \end{aligned} \tag{21}$$

Once the UA values are calculated, the global heat transfer coefficient, U, is needed in order to calculate the area, A. The global heat transfer coefficient depends on the steam and gas heat transfer coefficients, h_s and h_g respectively. These coefficients will be calculated in the next subsections.

2.2.5 Gas heat transfer coefficient

The gas heat transfer coefficient (h_g) is calculated with the Grimison correlations [33]. This calculation is performed only once in the pressure level, due to the minor variation of the properties of the gas.

$$h_g = \frac{Nu_g \cdot k_g}{d_g} \tag{22}$$

The Nusselt number, Reynolds numbers and some properties of the fluid need to be calculated.

$$Nu_g = 1.13 \cdot C1 \cdot Re_g^m \cdot Pr_g^{1/3} \tag{23}$$

Where $C1$ and m are constants depending on the outside diameter, transverse and longitudinal pitch (d_o, S_t and S_l). In this case, the requirements from Table 2 show that $S_t/d_o = S_t/d_o = 1.25$. According to [33] $C1 = 0.518$ and $m = 0.556$. Reynolds number is calculated as shown in Equation 24.

$$Re_g = \frac{\rho_g \cdot v_{max,g} \cdot d_o}{\mu_g} \tag{24}$$

The maximum velocity is calculated with Equation 25, knowing that is a staggered configuration, the following equation is valid.

$$\begin{aligned} v_{max,g} &= max\left(\frac{S_t \cdot v_g}{2 \cdot (S_d - d_o)}, \frac{S_t \cdot v_g}{S_t - d_o}\right) \\ S_d &= \sqrt{S_l^2 + \left(\frac{S_t}{2}\right)^2} \end{aligned} \tag{25}$$

Because the value of the velocity is not explicitly calculated, the gas mass flow is used along with the density. According to [35], the following equation can be used:

$$v_{max,g} \cdot \rho_g = \frac{M_g}{(S_t - d_o) \cdot N_r \cdot L_t} \tag{26}$$

The remaining properties are obtained with Coolprop.

$$\left.\begin{matrix} T1_g \\ P1_g \\ Air \end{matrix}\right\} \xrightarrow{\text{Coolprop}} \begin{matrix} k_g \\ \mu_g \\ Pr_g \\ \rho_g \end{matrix} \tag{27}$$

Once all these parameters are obtained, h_g is calculated.

2.2.6 Steam heat transfer coefficient

The procedure is fairly similar to h_g. However, in this case the Gnielinski equations are used [36]. The two phase conditions that take place in the evaporator have very complex calculations [37], that is the reason they are not in the scope of the project.

$$h_{s,x} = \frac{Nu_{s,x} \cdot k_{s,x}}{d_i} \tag{28}$$

$$Nu_{s,x} = \frac{\frac{f_{s,x}}{8} \cdot (Re_{s,x} - 1000) \cdot Pr_{s,x}}{1 + 12.7 \cdot \left(\frac{f_{s,x}}{8}\right)^{1/2} \cdot \left(Pr_{s,x}^{2/3} - 1\right)} \tag{29}$$

Where $f_{s,x}$ can be obtained using the Petukov correlations [19].

$$f_{s,x} = (0.790 \cdot \ln(Re_{s,x}) - 1.64)^{-2} \tag{30}$$

$$Re_{s,x} = \frac{\rho_{s,x} \cdot v_{s,x} \cdot d_i}{\mu_{s,x}} \tag{31}$$

Because the value of the velocity is not explicitly calculated, the gas mass flow is used along with the density. The following equation can be used.

$$v_{s,x} \cdot \rho_{s,x} = \frac{M_s}{N_{r,x} \cdot N_{c,x} \cdot \pi \cdot d_i^2} \tag{32}$$

The remaining properties are obtained with Coolprop. Mean pressure and temperature have been taken into account at the inlet and exit of every device.

$$\left.\begin{matrix} T_{m,s,x} \\ P_{m,s,x} \\ Water \end{matrix}\right\} \xrightarrow{\text{Coolprop}} \begin{matrix} k_{s,x} \\ \mu_{s,x} \\ Pr_{s,x} \\ \rho_{s,x} \end{matrix} \tag{33}$$

Finally, h_s is obtained.

The pressure drop values obtained from Table 2 need to be compared with the calculated ones in order to proceed with the calculations with confidence that the assumptions are correct. Pressure drop calculations are shown in Equation 34.

$$\begin{aligned} PD_{s,x} &= \frac{1}{2} \cdot v_{s,x}^2 \cdot \rho_{s,x} \cdot f_{s,x} \cdot \frac{L_t}{d_i} \\ v_{s,x} &= \frac{Re_{s,x} \cdot \mu_{s,x}}{\rho_{s,x} \cdot d_i} \end{aligned} \tag{34}$$

2.2.7 Global heat transfer coefficient

Once again, x denotes the superheater, evaporator and economizer. The conduction resistance has been neglected due to its small thickness and high thermal conductivity [38]. The gas heat transfer coefficient is shown below.

$$U_{g,x} = \left(\frac{d_o}{h_s \cdot d_i} + \frac{1}{h_g} \right)^{-1} \tag{35}$$

An alternative calculation is proposed in Equation 36 to calculate the steam global heat transfer coefficient.

$$U_{s,x} = \left(\frac{d_i}{h_g \cdot d_o} + \frac{1}{h_s} \right)^{-1} \tag{36}$$

2.2.8 Area

Finally, the area for the gas or steam side can be obtained.

$$A_{g,x} = \frac{UA_x}{U_{g,x}} \tag{37}$$

$$A_{s,x} = \frac{UA_x}{U_{s,x}} \tag{38}$$

2.2.9 Efficiencies

Efficiency for the HRSG (called effectiveness) and efficiency for the combined cycle is calculated according to [19]. For this project the values for the efficiency of the Brayton and Rankine cycle are set as $\eta_{Brayton} = 35\,\%$ and $\eta_{Rankine} = 44\,\%$.

$$\begin{gathered} \varepsilon_{HRSG} = \frac{Q}{Q_{max}} = \frac{M_s \cdot (H6_s - H1_s)}{M_g \cdot Cp_g \cdot (T1_g - T1_s)} \\ \eta_{CC} = \eta_{Brayton} + \varepsilon_{HRSG} \cdot \eta_{Rankine} \cdot (1 - \eta_{Brayton}) \end{gathered} \tag{39}$$

The full MATLAB® code for the HP is attached in subsection A.1.

2.2.10 Multi pressure

The calculations for the multi pressure model are done following the same procedure. In order to calculate the IP and LP areas, the gas pressure drops are needed. They are obtained as shown in Equation 40. X (correlation factor) and f_g (friction factor) are calculated from as explained in the external flow section in [19]. For the geometric properties of this model, $X \simeq 1$ and $f_g \simeq 0.2$. The number of columns correspond to the total number of columns within the pressure level.

$$\begin{aligned} PD_g &= N_{c,x} \cdot X \cdot \frac{v_g^2 \cdot \rho_g}{2} \cdot f_g \\ v_g &= \frac{Re_g \cdot \mu_g}{\rho_g \cdot d_i} \end{aligned} \tag{40}$$

Another relation must be included in the code in order to obtain temperatures $T14s$ and $T8s$. According to [30], the terminal temperature difference (TTD) is the difference between the inlet gas exhaust temperature and the outlet superheated steam. It is set at 25 °C.

$$\begin{aligned} T14s &= T4g - TTD \\ T8s &= T7g - TTD \end{aligned} \tag{41}$$

The full MATLAB® code for the multi pressure is attached in subsection A.3.

2.3 Optimization

The previous calculation allowed the code to obtain the area of the HRSG given some particular requirements. However, this code takes a step further and optimizes the solution. Several studies have been carried out to optimize the HRSG in the past.

- Franco *et al* [12] focused on the minimization of pressure losses and compactness.
- Casarosa *et al* [21] took into account the exergy losses of the system. The exergy method allows the localization of the most ineficient components of the system [39].
- Valdes *et al* [22] and Duran *et al* [40] proposed a thermoeconomic model to identify the most relevant parameters taking into consideration the areas with higher economic losses.
- Soo *et al* [41] optimized the power plant using a genetic algorithm.
- Manassaldy *et al* proposed a non linear method to optimize net power output, weight ratio and net heat transfer [39].

All these authors took into account their own parameters, neglecting others. My proposal takes into consideration all the calculations from the very beginning and shows all the operations made as described in subsection 2.2. Furthermore, the input parameters can be changed as desired and the model will optimize the output the same way. The model proves to be flexible as it will be revealed because single, double and triple pressure CCPP can be modeled. In this subsection 2.3 only the single pressure level will be taken into consideration. The model is optimized with MATLAB®. The tool used for this process is *fmincon* [42]. It is a nonlinear programming solver that minimizes a given function $f(x)$. The parameters involved are the following:

Input	Description
fun	Function to minimize
x_0	Initial point
$A \cdot x \leq b$	Linear inequality constraints
$Aeq \cdot x \leq beq$	Linear equality constraints
$lb \leq x \leq ub$	Lower and upper bounds
$xval$	Objective function value at solution
$nonlcon$	Nonlinear constraints
$c(x) \leq 0$	Nonlinear inequality constraints
$ceq(x) = 0$	Nonlinear equality constraints
x	Solution

Table 3: Parameters for *fmincon*

The function to minimize is the area of the HRSG. Either Equation 37 or Equation 38 can be chosen. The definition of the MATLAB® tool requires the function to be in terms of the solution vector x. Therefore, the calculations mentioned in subsection 2.2 are inserted at the end of the code as a function, as shown in Equation 42.

$$
\begin{aligned}
&function f = Opti\_Fun(x)\\
&\%\% \text{ Input Data}\\
&\%\% \text{ Gas Properties}\\
&M_g = 650\\
&T1_g = 886\\
&P1_g = 101.3 \cdot 10^3\\
&etc...
\end{aligned}
\tag{42}
$$

There are no constraints associated to linear or nonlinear equalities and inequalities. Therefore, the values are empty.

Parameter	Value
A	[ ]
b	[ ]
Aeq	[ ]
beq	[ ]
$nonlcon$	[ ]

Table 4: Value for A, b, Aeq, beq and $noncol$ for $fmincon$

The syntax of the MATLAB® structure is the following:

$$[x, fval, exitflag, output] = fmincon(fun, x0, A, b, Aeq, beq, lb, ub, nonlcon, options) \tag{43}$$

Where $(fun, x0, A, b, Aeq, beq, lb, ub, nonlcon, options)$ are the input parameters and $[x, fval, exitflag, output]$ are the output parameters. At this phase, the problem relies on the selection of variables, along with the initial values, lower and upper bounds. This is the critical step of the optimization due to the great amount of possible variables to optimize. As it is shown from literature, AP and PP appear to be important parameters influencing the final output of the CCPP. The total length is also a significant factor due to the involvement in the calculation of h_g. Additionally, the number of total tubes greatly determine the size of the HRSG and the materials used in the construction, therefore the total cost of the CCPP. These are the selected variables, they are stored in the vector x. As shown in Table 5, the initial value, lower and upper bounds are included according to the most typical literature values.

x	Variable	$x0$	lb	ub
$x(1)$	AP	15	5	25
$x(2)$	PP	15	5	20
$x(3)$	L_t	15.3	10	20
$x(4)$	$N_{c,SH}$	10	4	12
$x(5)$	$N_{c,EV}$	10	4	12
$x(6)$	$N_{c,EC}$	10	4	12
$x(7)$	$N_{r,SH}$	10	4	12
$x(8)$	$N_{r,EV}$	10	4	12
$x(9)$	$N_{r,EC}$	10	4	12

Table 5: Solution vector x

The options selected for the optimization are the following.

- 'Display' = 'notify' It will display output only if the function does not converge.
- 'Algorithm' = 'sqp' The default 'interior-point' algorithm failed because it had an negative output for the function. According to the suggestions found in [43], the 'sqp' method is used.
- 'PlotFcn',@optimplotfvalue. This option plots the function value while the algorithm executes.

After the single pressure optimization, the optimized results for the selected variables will be used for the multi pressure calculations. Therefore, the multi pressure model will be calculated based on a minimized area.

Finally, off-design calculations are performed based on the multi pressure code.

3 Results

This section presents the outcome of the previous calculations. Analysis and explanation of all figures will be presented. These results have been obtained using the MATLAB® software.

3.1 Results for single pressure model

Results and optimization of the single pressure HRSG model are presented.

Q[MW]	A_g[m^2]	A_s[m^2]	ϵ_{HRSG}[%]	η_{CC}[%]
216.6	20827.1	19648.2	66.19	53.93

Table 6: Single pressure results

Heat transfer is found to be 217 MW a reasonable value for an HRSG. However, **area** appears to be of considerable size (20 827 m^2). This is the reason for the optimization presented in Table 7. Regarding **HRSG effectiveness**, values range from 60 % to 85 % according to [38] depending on the pressure and temperature inlets from the exhaust gases. Therefore, the model remains within the usual limits. **CC efficiency**, as it was stated before ranges from 55 % from 60 %. The slightly lower value is due to the fact that this is a single pressure model. As it will be seen later, the multi pressure model provides a higher efficiency.

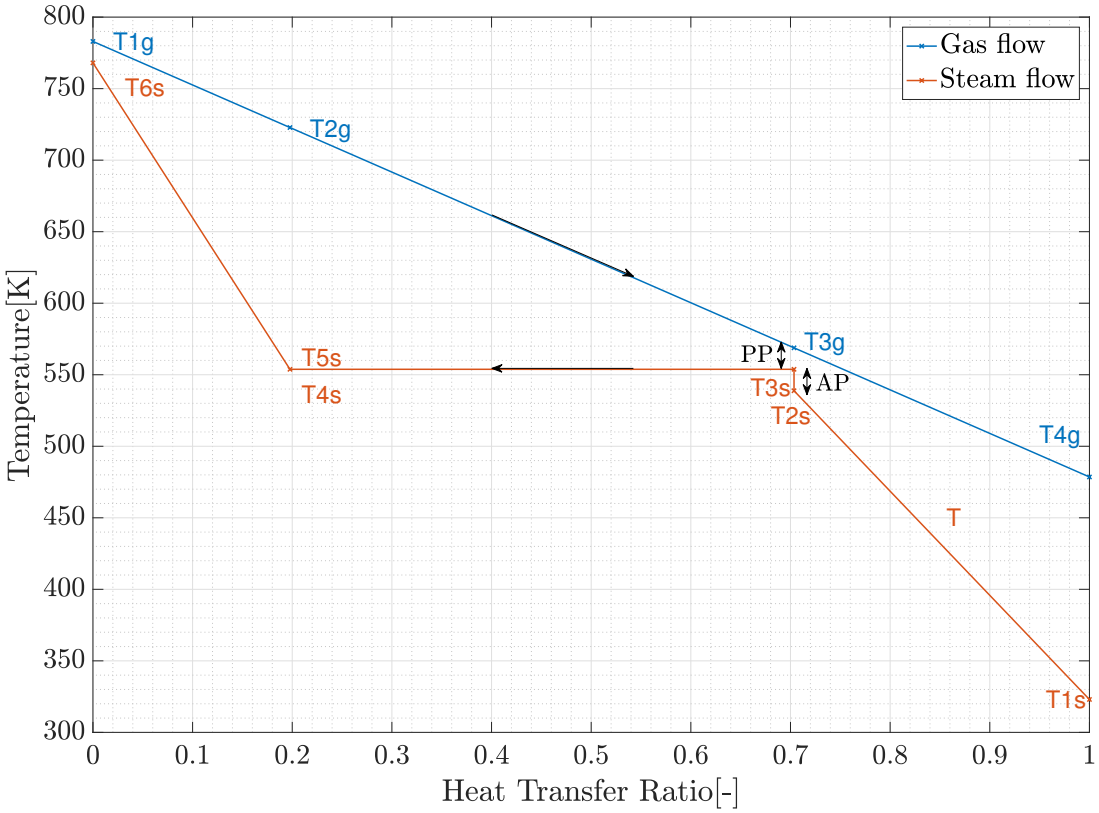

Figure 17: Single pressure temperature profile results

Figure 17 shows the temperature profile of the HRSG. AP and PP are represented in the graph. The shape of the profile is the one encountered in all HRSG examples.

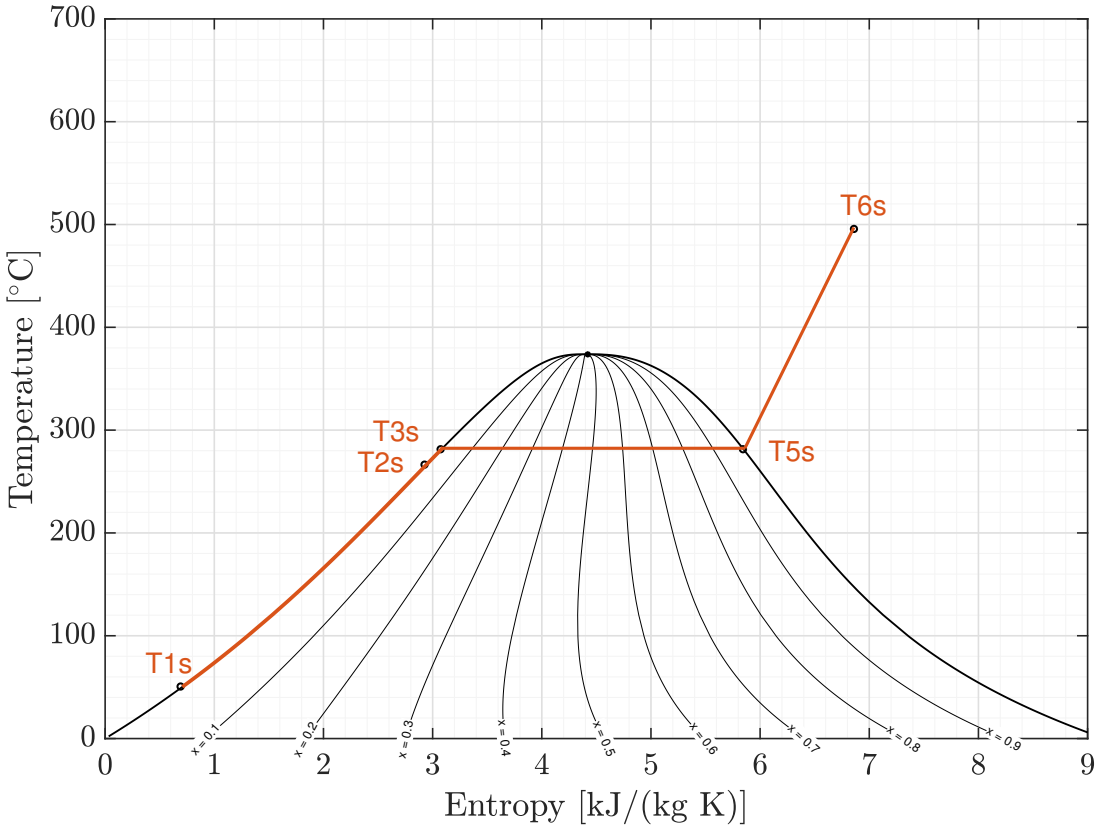

Figure 18: Single pressure T-S Diagram results

$T-S$ diagram is shown for the single pressure model. As it can be seen, the location of the steam points correspond with accuracy with the assumptions made along the project.

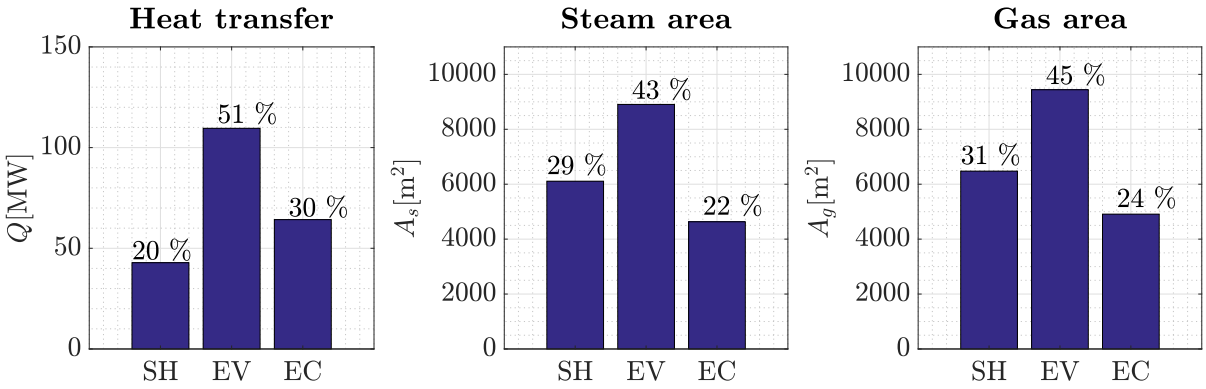

Figure 19: Single pressure gas results

Heat transfer and area distribution across the HRSG elements is presented in Figure 19. Heat transfer percentages values are not found in literature, therefore, they can not be compared. Concerning area percentages, they are similar to those found in scientific papers. $A(SH) = 10\,\%$, $A(EV) = 50\,\%$ and $A(EC) = 40\,\%$ is recommended according to [22]. Results are not far from those values, only that the SH area is larger, it is mainly because of the relatively low $T1_g$ selected for the model compared to the [22] input values. If $T1_g$ is increased, the percentage of SH decreases and the percentage of EC decreases. For example, if $T1_g = 850\,\text{K}$, then $A(SH) = 17\,\%$, $A(EV) = 45\,\%$ and $A(EC) = 32\,\%$. This indicates the validity of this project.

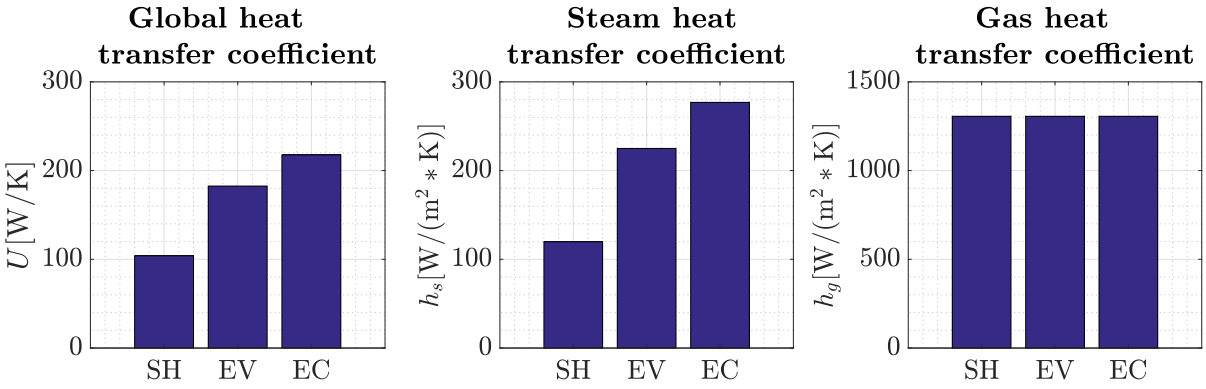

Figure 20: Single pressure steam results

With regard to Figure 20, the gas heat transfer coefficients, h_g, are equal because the gas properties across the sections of the HRSG are approximately the same. On the other hand, steam heat transfer coefficients, h_s do change. As it was seen in subsubsection 2.2.6, Reynolds number, Re, strongly depends on the viscosity of the fluid, μ, because all the other factors remain constant. It is found from the code that viscosity decreases going from EC to SH, in fact, $\mu_{s,SH} = 2.387 \cdot 10^{-5}\,\mathrm{Pa\,s}$, $\mu_{s,SH} = 1.865 \cdot 10^{-5}\,\mathrm{Pa\,s}$ and $\mu_{s,SH} = 1.747 \cdot 10^{-5}\,\mathrm{Pa\,s}$. This property explains the results obtained for h_s. Global heat transfer coefficient, U, is coherent with the h_s values, larger in the EC and smaller in the SH.

Reviewing pressure drops in the steam side of the HRSG, it was found that those percentages were much lower than the initial values. However, we estimate that this values could increase in the future due to sediment accumulation or other reasons. Taking this into consideration accomplishes a safer model from a long term point of view.

3.2 Optimization of a single pressure model

Once the calculation of the single pressure model is obtained, the **optimization** can be applied.

Q_{opt}[MW]	$A_{g,opt}$[m^2]	$A_{s,opt}$[m^2]	$\epsilon_{HRSG,opt}$[%]	$\eta_{CC,opt}$[%]
207 (-5%)	4928 (-76%)	4649 (-76%)	63.24 (-2.95%)	53.09 (-0.84%)

Table 7: Single pressure optimization results

Results show that the optimization minimized the area from 20 827 m^2 to 4928 m^2. This huge different is obtained with the MATLAB® optimization as described in previous sections. A decrease of 76 % implies a massive reduction of the acquisition cost of the materials for the HRSG, therefore a reduction of the total cost of the CCPP. It also implies the construction of a smaller HRSG, in case the space requirements are very strict for the power plant. Nevertheless, this decrease in area also involves a lower heat transfer (4 %), HRSG effectiveness (3 %) and CC efficiency (1 %).This project is focused on area reduction, which is done by a large amount, therefore they are a feasible consequence of the area minimization.

x	Variable	Value
$x(1)$	AP	25
$x(2)$	PP	20
$x(3)$	L_t	10
$x(4)$	$N_{c,SH}$	4
$x(5)$	$N_{c,EV}$	4
$x(6)$	$N_{c,EC}$	4
$x(7)$	$N_{r,SH}$	4
$x(8)$	$N_{r,EV}$	4
$x(9)$	$N_{r,EC}$	4

Table 8: Single pressure optimized values for vector x

Optimized values make clear that the maximum value of pinch point and approach point must be selected. Also, regarding the length and the number of tubes, the minimum value is chosen. These maximum and minimum values come from the lower and upper bounds set in Table 5. Hence, it reflects the importance of selection of references in the project.

3.3 Results for multi pressure calculations

Taking into account results from the single pressure optimization Table 7, the values for the inputs are modified in order to minimize the area of heat transfer (A) in the multi pressure model. Where x in $N_{c,x,HP}$ stands for SH,EV and EC.

Description	Parameter	Value	Unit	Reference
HRSG properties	AP_{HP},AP_{IP},AP_{LP}	25	K	[29]
	PP_{HP},PP_{IP},PP_{LP}	20	K	[29]
	TTD	25	K	[30]
Gas properties	M_g	650	kg/s	[30]
	$T1_g$	886	K	[30]
	$P1_g$	1.013	bar	[30]
Steam properties	$T20_s$	798	K	[30]
	$T15_s$	525	K	[44]
	$T9_s$	420	K	[44]
	$T3_s$	323	K	[31]
	$P20_s$	200	bar	[30]
	$P14_s$	80	bar	[30]
	$P8_s$	2	bar	[30]
	$PD_{s,SH}$	8	%	[32]
	$PD_{s,EV}$	0	%	–
	$PD_{s,EC}$	25	%	[32]
	$X19s, X13s, X7s$	1	–	–
Geometric properties	L_t	10	m	[30]
	d_o	53	mm	[31]
	d_i	50	mm	[31]
	S_t,S_l	66	mm	[33]
	$N_{c,x,HP}$	4	–	[45]
	$N_{r,x,HP}$	4	–	[45]
	$N_{c,x,IP}$	4	–	[45]
	$N_{r,x,IP}$	4	–	[45]
	$N_{c,x,LP}$	4	–	[45]
	$N_{r,x,LP}$	4	–	[45]
CC properties	$\eta_{Brayton}$	35	%	-
	$\eta_{Rankine}$	44	%	-

Table 9: Multi pressure input data

$\boldsymbol{Q_{opt,3P}}$[MW]	$\boldsymbol{A_{g,opt,3P}}$[m^2]	$\boldsymbol{A_{s,opt,3P}}$[m^2]	$\boldsymbol{\epsilon_{HRSG,opt,3P}}$[%]	$\boldsymbol{\eta_{CC,opt,3P}}$[%]
341.9 (+58%)	15634.1(-22%)	14749.1(-22%)	83.57(+17%)	58.90(+5%)

Table 10: Multi pressure results

Final results are obtained for the multi pressure model in Table 10. In comparison with the values obtained in the first calculation from Table 6, results are outstanding. **Heat transfer** is increased by a 58 %. **Area** is significantly reduced (25 %), once again, reducing overall costs. **HRSG effectiveness** increases up to 83.57 % due to the improvements regarding heat losses. Finally, **CC efficiency** grows up to 58.90 %.

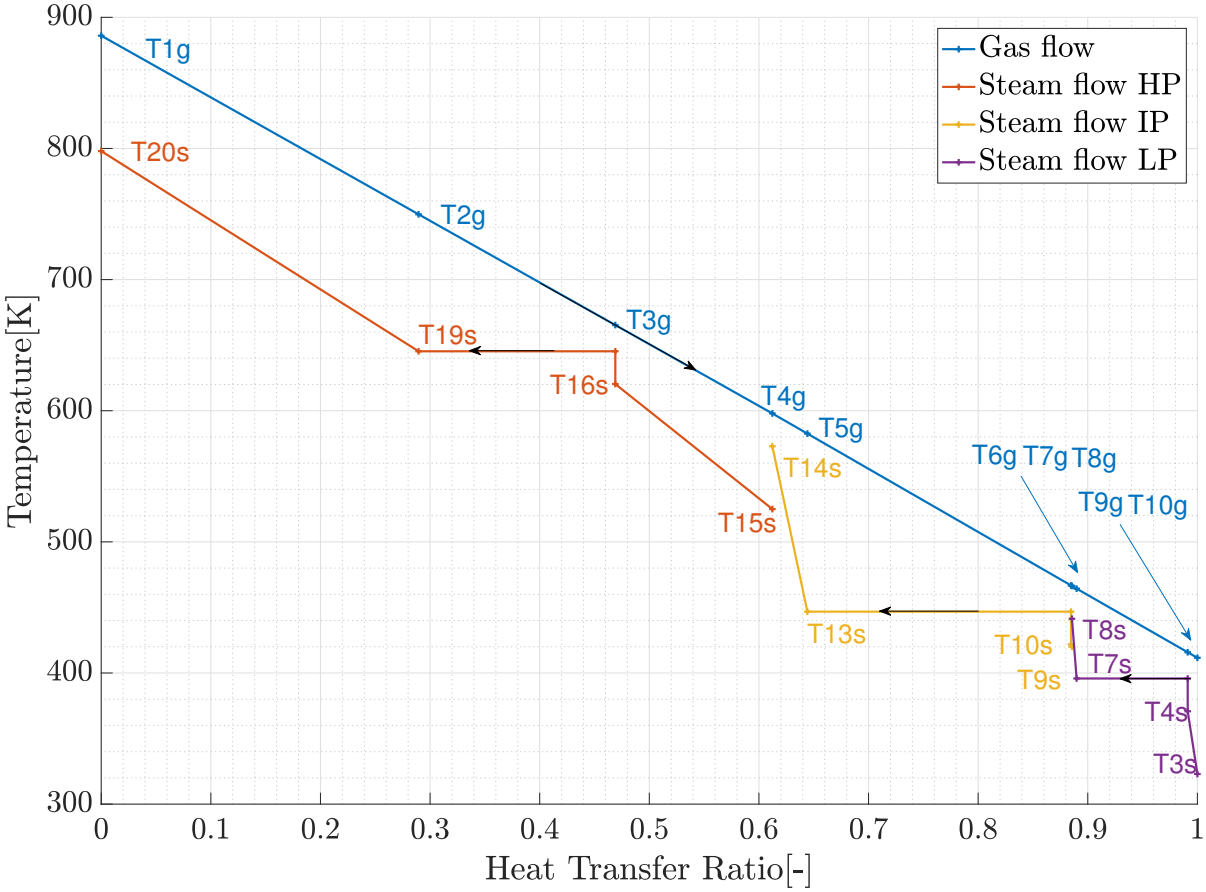

Figure 21: Multi pressure temperature profile results

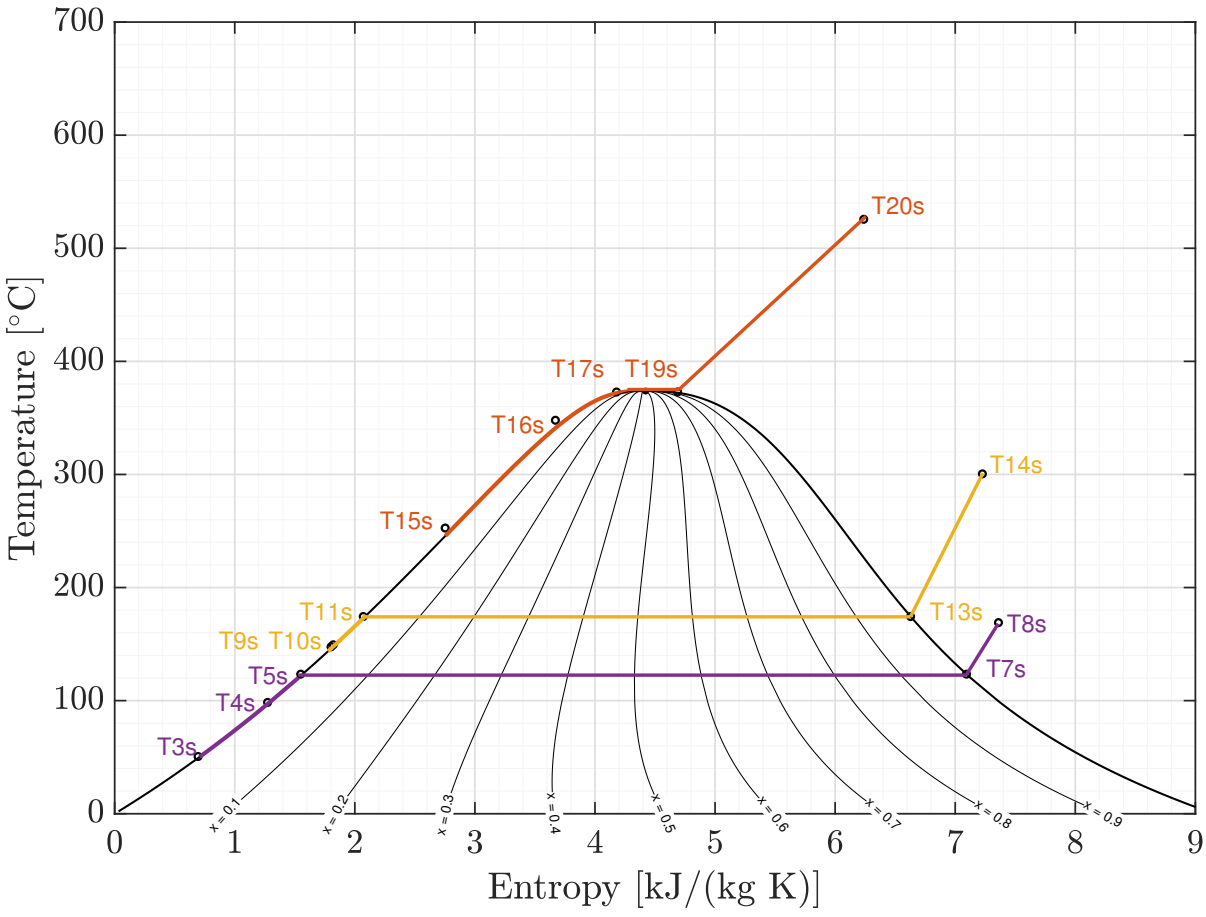

Figure 22: Multi pressure T-S Diagram results

Temperature profile (Figure 21) is very similar to those found in literature. It is clear that HP takes most of the heat transfer with a temperature difference of $\simeq 400\,\mathrm{K}$. On the other hand, IP and LP only have a temperature difference of $\simeq 200\,\mathrm{K}$ and $\simeq 100\,\mathrm{K}$ respectively. Figure 22 shows the $T-S$ diagram for the multi pressure level.

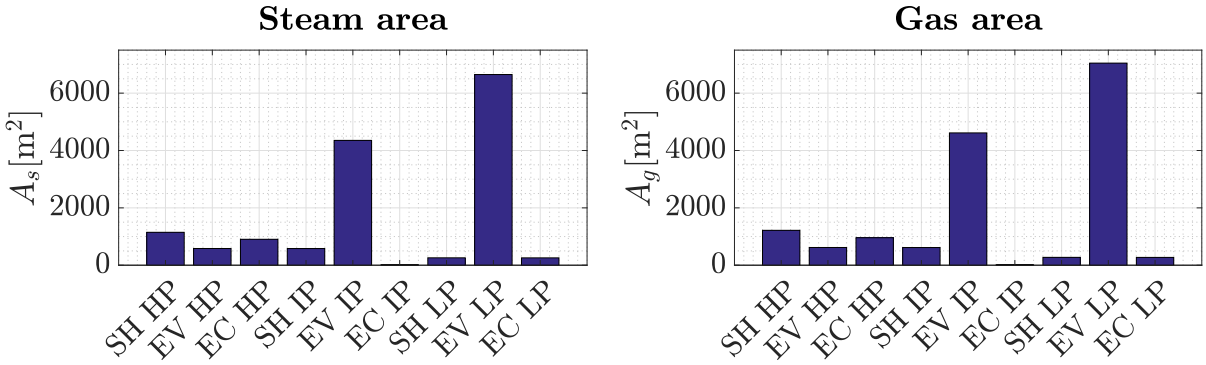

Figure 23: Multi pressure area results

Results for the **area** (Figure 23) show that evaporators in IP and LP need a big area to transfer heat from the gas to the steam cycle. The main cause are phase changes, because they need a large amount of energy to take place. At high temperatures ($\simeq 650\,\mathrm{K}$) and pressures ($\simeq 216\,\mathrm{bar}$), as it occurs in the HP level, less heat is required to perform the heat exchange.

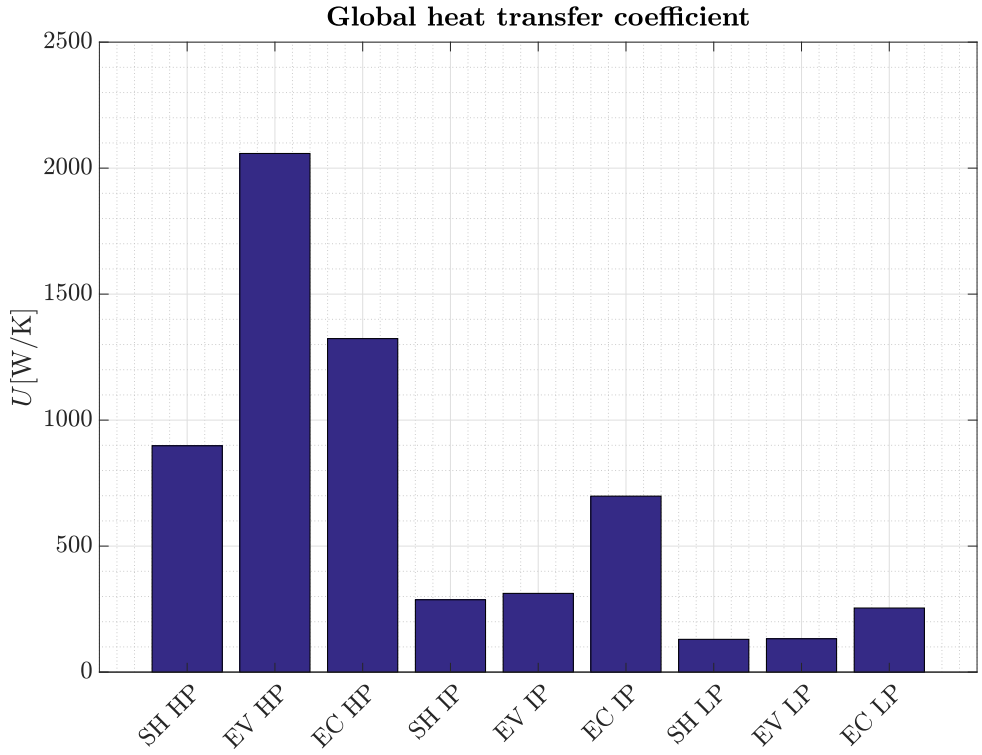

Figure 24: Multi pressure global heat transfer coefficient results

Global heat transfer coefficient is discovered to be higher in the HP level. This is expected because the larger the value of U, the smaller the area and the greater the heat transfer, according to Equation 6. In the lower pressure levels the opposite conditions take place.

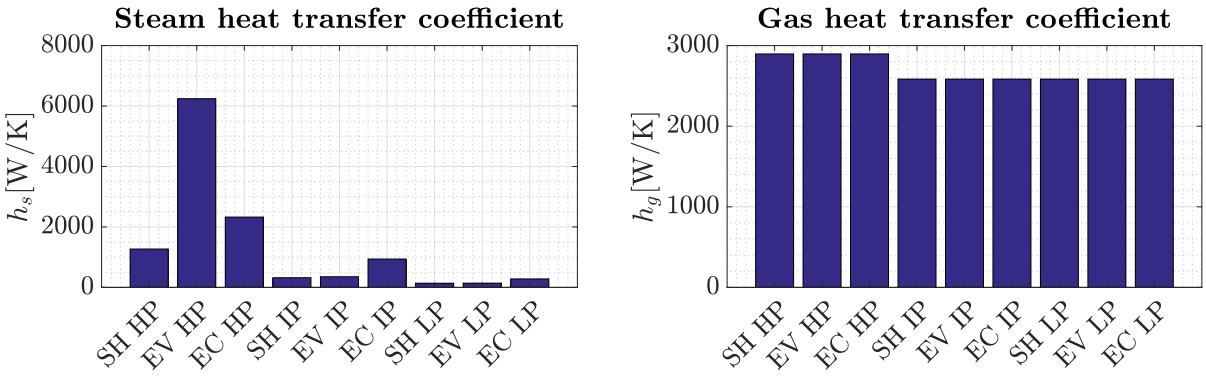

Figure 25: Multi pressure steam and gas heat transfer coefficients results

Steam heat transfer coefficient to a certain degree depends on the properties as it was explained in subsection 2.2. The values considerably vary across the HRSG. The largest h_s is found in the $EV\ HP$. Running a few simulations, it was found that it is because of the large value of constant pressure specific heat, $Cp_{s,EV,HP}$ in those high temperature and high pressure conditions. **Gas heat transfer coefficient** maintain their value predominantly because the gas properties differ in a small amount. These values of gas coefficients do not have much influence in the global heat transfer coefficient, U. It can be deduced that h_s has more impact on the overall area calculations.

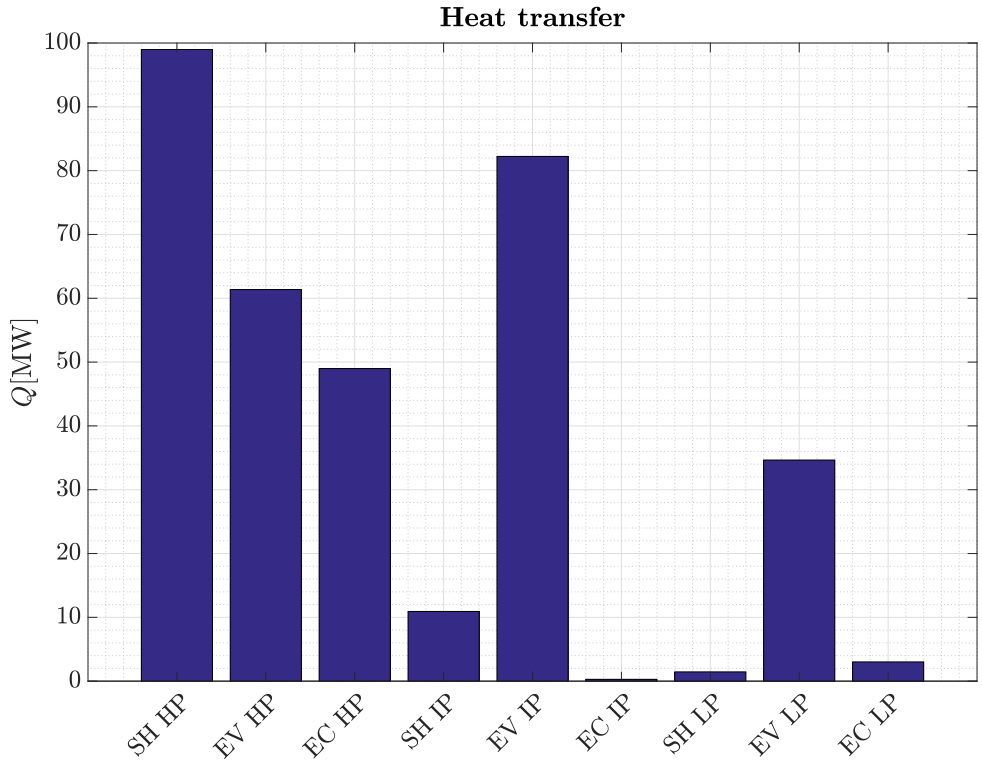

Figure 26: Multi pressure heat transfer results

Finally, regarding **heat transfer**, Q, most of it is originated in the HP level. This is because the large difference of temperature and the large global heat transfer coefficient. The evaporator in IP and LP also produce a considerable amount of heat transfer due to the change of phase. As it was stated in [38], the maximum heat transfer is produced in the EV for the high pressure level and in the EC for the low pressure level. These results can be considered as validation for the model.

3.4 Off-design results for multi pressure calculations

So far, the model of HRSG was optimized for specific input parameters. However, when those variables change there is no data available on how the CCPP is going to behave. That is why the model takes a step further and studies how the HRSG operates as a result of the modification of input data. A sensitivity analysis is performed with the multi pressure CCPP. Heat transfer, area, HRSG efficiency and CC efficiency will be the output results. The optimized variables such as approach point, pinch point, length of tubes and number of tubes remain unchanged in this subsection. Table 11 shows the variables taken into consideration and their range. Gas mass flow (M_g), HRSG gas inlet temperature ($T1_g$) and HRSG water outlet temperature ($T20_s$) are important parameters, because they are the most likely to be modified during the lifetime of the CCPP. Values from previous calculation are shown as '$*$'.

Variable	Range	Unit
M_g	$500 - 700$	kg/s
$T1_g$	$790 - 990$	K
$T20_s$	$690 - 890$	K
$P20_s$	$180 - 240$	bar

Table 11: Off-design variables

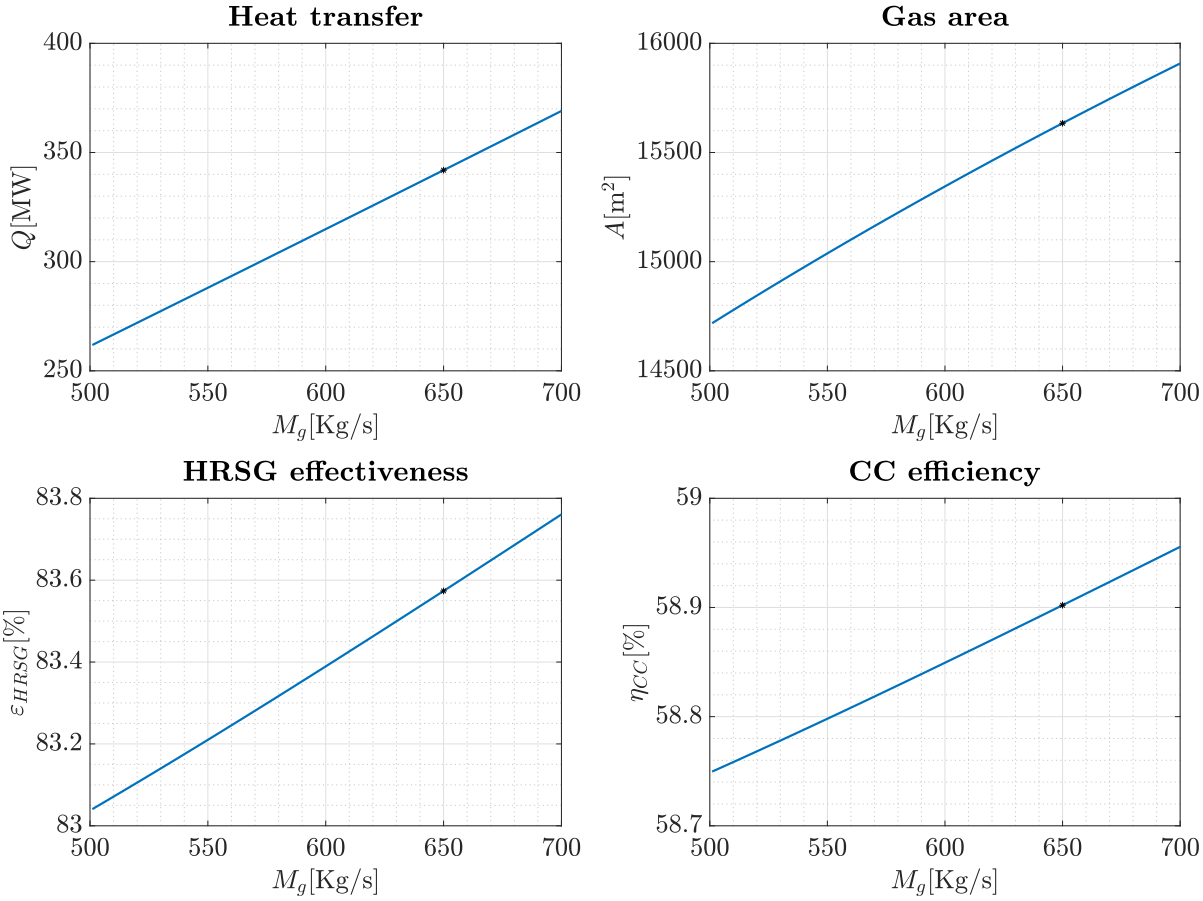

Figure 27: Off design evolution for M_g

Heat transfer depends on the gas mass flow as shown in Equation 16, therefore it will increase if M_g does. Furthermore, **area** increases if heat transfer does, as shown in subsection 2.2. Figure 27 also shows that M_g affects in the **HRSG effectiveness** and **CC efficiency** in the same way. This is because these two variables depend on temperatures

and gas flows. Temperatures remain unchanged, however, gas flow does vary, therefore ε_{HRSG} and η_{CC} also increase with M_g.

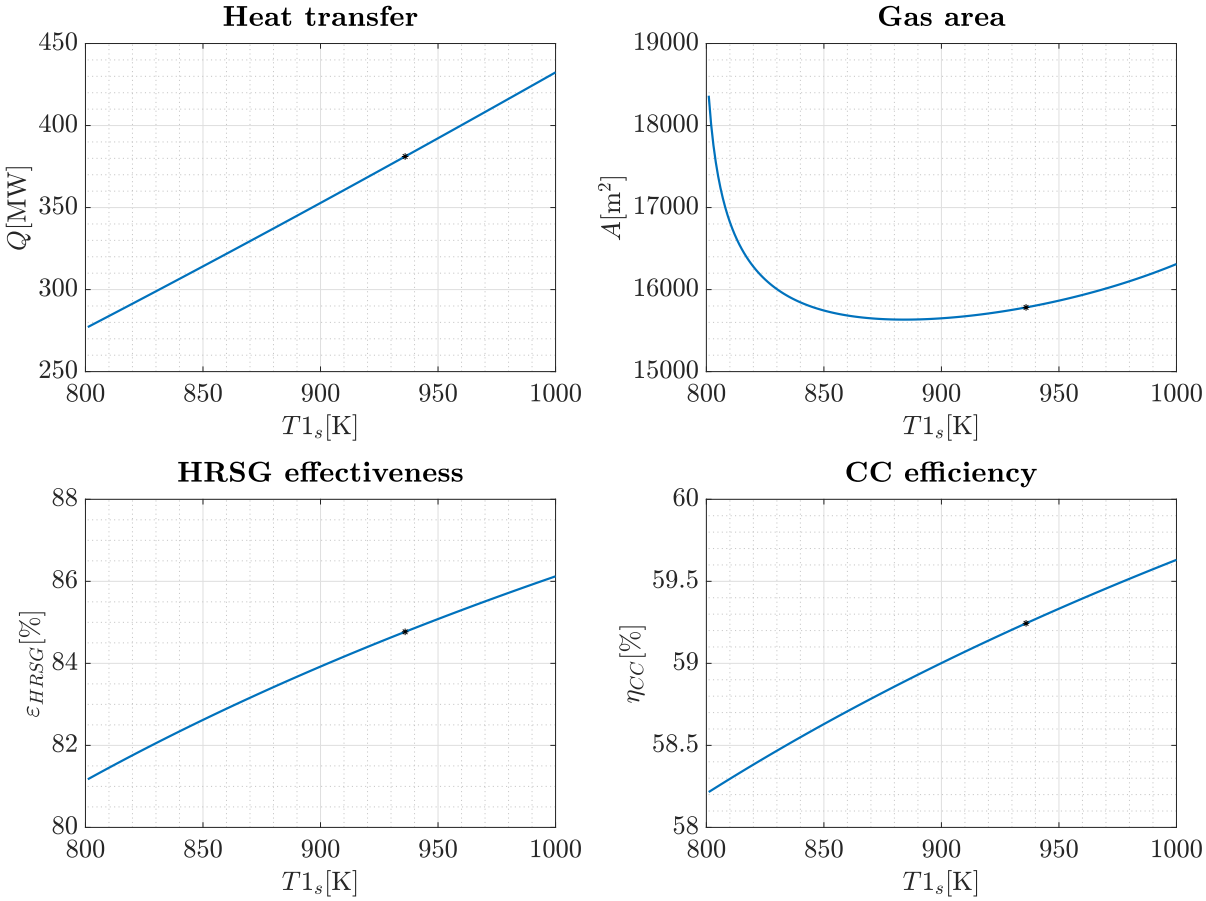

Figure 28: Off design evolution for $T1_g$

Heat transfer, **area**, **HRSG effectiveness** and **CC efficiency** increase if the gas exhaust temperature increases. It is explained again by Equation 16. This is the main goal of the latest HRSG designs, as explained in subsection 1.2.5. Nowadays, the limitation of $T1_g$ is found in the maximum temperature that the turbine blades can endure. An important remark, in the area graph an asymptotic behavior is found. This makes absolute sense because the inlet temperature, $T1_g$, can never be smaller than the steam turbine inlet temperature, $T20_s$.

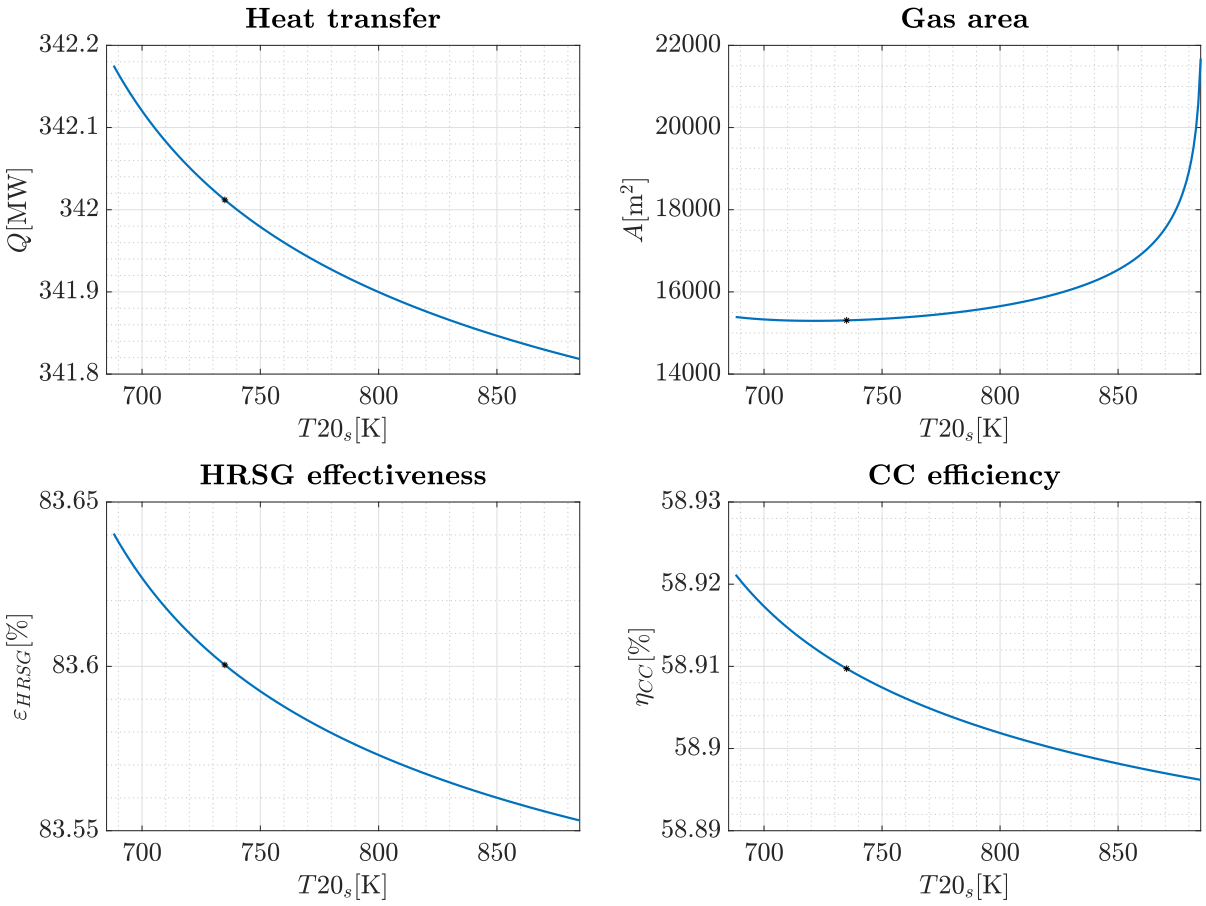

Figure 29: Off design evolution for $T20_s$

As it is shown in Figure 29, increasing $T20_s$ is not beneficial for any of the studied variables. When this value increases, the temperature difference between $T20_s$ and $T1_g$ reduces, therefore the **heat transfer** does as well. This produces a lower **HRSG effectiveness** and **CC efficiency**. **Area** calculation follows the same outcome. There is also an asymptote when $T20_s$ surpasses $T1_g$, as expected.

4 Economic Study

The economic impact that this project would have in a real power plant is presented in this section. Equation 44 shows an estimation of the money savings that this model can provide. Assuming that power output is $W_{cycle} = 350\,\text{MW}$ and the power plant works approximately $T = 6000\,\text{h/year}$. The average natural gas price in 2016 was $C_{gas} = 15\,€/(\text{MW h})$ [46]. Moreover, taking into account results from Table 12 and using the definition of efficiency for any cycle (Equation 1), the total cost of the fuel per year is presented in Equation 44.

$$\begin{aligned} Cost_{fuel} &= Q_{in} \cdot C_{gas} \cdot T = \frac{W_{cycle}}{\eta_{CC}} \cdot C_{gas} \cdot T \\ Cost_{fuel,1P} &= \frac{350\,\text{MW}}{0.5393} \cdot \frac{15\,€}{1\,\text{MW h}} \cdot \frac{6000\,\text{h}}{1\,\text{year}} = 58\,409\,049\,€/\text{year} \\ Cost_{fuel,3P} &= \frac{350\,\text{MW}}{0.5890} \cdot \frac{15\,€}{1\,\text{MW h}} \cdot \frac{6000\,\text{h}}{1\,\text{year}} = 53\,480\,475\,€/\text{year} \\ Savings &= 58\,409\,049\,€/\text{year} - 53\,480\,475\,€/\text{year} = 4\,928\,574\,€/\text{year} \end{aligned} \tag{44}$$

A 5 % increase in efficiency implies 4 928 574 € of savings per year. This is a huge amount for a relatively small power plant ($\simeq$ 350 MW). Considering a larger power plant such as the one in Lumut, Malaysia (with $\simeq$ 1300 MW) of power output [27]), the improvements are even better (around 18 306 130 € of savings per year).

5 Conclusion

HRSG design involves numerous parameters to be studied. This model performs the calculations providing tables and graphic results within seconds. In addition, it automatically makes an optimization for the initial situation. Finally, it executes a sensibility analysis for off-design conditions. Furthermore, it does not require large computational resources.

It is important to remark the flexibility of the model. Input data can be easily modified in order to adapt the model to any specific requirements. Contemplating a mid-long term period, the code will be still valid in the future with some minor modifications. As it was stated before, state of the art focuses on two main areas of development to enhance CC overall efficiency. Cooling blade technology will increase the exhaust gas temperature in order to improve the cycle. Additionally, regarding the HRSG, the inclusion of reheat, more than 3 pressure levels and improvements regarding heat losses will be changes that will happen sooner or later in the industry. This model will allow those changes to be assessed and studied in a faster and more reliable way.

This model performs four main calculations: single pressure model, optimization, multi pressure model and off design. All of these calculations are done in the SH, EV and EC for the high, intermediate and low pressure level. This implies that any property such as temperature, pressure, density , viscosity, etc, of the both gas and steam can be obtained easily. Any problem existing in the HRSG could be avoided or mitigated if the location of the problem is properly defined. Furthermore, those properties of the fluids across the tubes can be used for other studies such as mechanical stress, strain, fatigue or failure. In order to make a summary of the results, Table 12 is shown.

$\boldsymbol{Q}$[MW]	$\boldsymbol{A}$[m^2]	$\boldsymbol{A}$[m^2]	$\boldsymbol{\epsilon_{HRSG}}$[%]	$\boldsymbol{\eta_{CC}}$[%]
$\boldsymbol{1P}$	217	20827	66.19	53.93
$\boldsymbol{Opt}$	207 (-5%)	4928 (-76%)	63.24 (-2.95%)	53.09 (-0.84%)
$\boldsymbol{Opt, 3P}$	342(+58%)	15634(-25%)	83.57(+17.38%)	58.90(+4.97%)

Table 12: Summary of results

The MATLAB® model proposed in this project is found to be quite effective and powerful. The **single pressure model** revealed a large area of heat transfer. Then, **optimization** procedures significantly improved results. As it was explained before, the optimization algorithm made the variables to converge to their upper or lower limits in order to minimize the area. Those variable constraints were found in distinguished articles about HRSG's. As for the **multi pressure model**, it remarkably decreased (25 %) the area of heat transfer and impressively increased heat transfer rates, HRSG effectiveness and CC efficiency. **Off-design calculations** were quite useful because the CCPP does not always work at full load. At partial loads, it is complicated to estimate how the plant is going to behave. If the gas exhaust conditions change, the overall performance of the HRSG also changes. This model provides an estimation of those changes. Additionally, it allows the possibility of comparing the performance of different gas turbine suppliers.

As it was stated in section 3, results are fairly similar to those found in literature. This validates the model and proves the success of this project. Another conclusion that can be deduced from is that more surface does not always imply more heat transferred. Exactly the same conclusion that Ganapathy came up with in his article [47]. This fact is an additional evidence corroborating this model.

6 Future projects

As it was explained, this project took into consideration some basic assumptions. In future projects related to this one, the following course of action could be applied.

- This project assumed the Gnielinski equations for the evaporator because of the complexity of the byphasic correlations. More parameters and further studies are needed in order to perform those calculations presented by Klimenko [37].
- Bare tubes were selected for this project. However, most HRSG's have fins. Solid or segmented fins could be included. This addition implies more variables and parameters that change the gas heat transfer coefficient correlations.
- Nine variables were selected for the optimization. More variables could be chosen to minimize the area of the heat exchanger. Some interesting parameters that could be included are inside diameter, d_i, outside diameter, d_o, longitudinal pitch, S_l, or transverse pitch, S_t.
- Companies won't provide any real data of CCPP because of obvious confidentiality and commercial reasons. However, it could be negotiated with them taking into consideration a more professional standpoint (e.g. for a scientific paper).
- Reheat after the HP level could be added in order to increase the efficiency.
- Optimization of the code could also be implemented. Additionally an user interface could be added to the model.

References

[1] BP, "Statistical Review of World Energy Underpinning Data 1965-2016," accessed 2017-08-08. [Online]. Available: http://www.bp.com/en/global/corporate/energy-economics/statistical-review-of-world-energy/downloads.html

[2] P. Sindareh-Esfahani, E. Habibi-Siyahposh, M. Saffar-Avval, A. Ghaffari, and F. Bakhtiari-Nejad, "Cold start-up condition model for heat recovery steam generators," *Applied Thermal Engineering*, vol. 65, no. 1, pp. 502–512, 2014.

[3] REE, "Operación Sistema Eléctrico," accessed 2017-08-09. [Online]. Available: http://www.ree.es/es/actividades/operacion-del-sistema-electrico

[4] U. Nations, "Kyoto Protocol," accessed 2017-08-09. [Online]. Available: http://unfccc.int/kyoto_protocol/items/2830.php

[5] BP, "Statistical Review of World Energy 2017," accessed 2017-08-09. [Online]. Available: http://www.bp.com/content/dam/bp-country/es_es/spain/documents/downloads/PDF/ULTIMA_INFOGRAFIA_INFORME_BP_SR17.pdf

[6] REE, "El Sistema Eléctrico Español 2016," accessed 2017-08-09. [Online]. Available: http://www.ree.es/sites/default/files/11_PUBLICACIONES/Documentos/InformesSistemaElectrico/2016/inf_sis_elec_ree_2016.pdf

[7] K. Saidi and M. B. Mbarek, "Nuclear energy, renewable energy, co_2 emissions, and economic growth for nine developed countries: Evidence from panel granger causality tests," *Progress in Nuclear Energy*, vol. 88, pp. 364 – 374, 2016. [Online]. Available: http://www.sciencedirect.com/science/article/pii/S014919701630018X

[8] I. Piccirilli Dorsey, "Fossil fuels — eesi," 2017. [Online]. Available: http://www.eesi.org/topics/fossil-fuels/description

[9] 2017. [Online]. Available: http://needtoknow.nas.edu/energy/energy-sources/fossil-fuels/coal/

[10] M. J. Moran and H. N. Shapiro, *Fundamentals of engineering thermodynamics*, 5th ed. Wiley, 2004.

[11] T. K. Ibrahim and M. M. Rahman, "Effect of compression ratio on performance of combined cycle gas turbine," *International Journal of Energy Engineering*, vol. 2, no. 1, 2012.

[12] A. Franco, "Analysis of small size combined cycle plants based on the use of supercritical HRSG," *Applied Thermal Engineering*, 2011.

[13] J.-Y. Shin, Y.-S. Son, M.-G. Kim, J.-S. Kim, and Y.-J. Jeon, "Performance analysis of a triple pressure HRSG," *KSME International Journal*, vol. 17, no. 11, pp. 1746–1755, 2003.

[14] T. Srinivas, "Thermodynamic modelling and optimization of a dual pressure reheat combined power cycle," *Sadhana*, vol. 35, no. 5, pp. 597–608, 2010.

[15] G. V, *Industrial Boilers and Heat Recovery Steam Generators*. Taylor and Francis Group, 2002.

[16] A. Bassily, "Modeling, numerical optimization, and irreversibility reduction of a dual-pressure reheat combined-cycle," *Applied energy*, vol. 81, no. 2, pp. 127–151, 2005.

[17] T. Wahlberg, "Modeling of heat transfer," 2011.

[18] J. L. Rapún Jiménez, "Modelo matemático del comportamiento de ciclos combinados de turbinas de gas y vapor," Ph.D. dissertation, Industriales, 1999.

[19] T. L. Bergman and F. P. Incropera, *Fundamentals of heat and mass transfer*. John Wiley, 2011.

[20] T. K. Ibrahim and M. M. Rahman, "Study on effective parameter of the triple-pressure reheat combined cycle performance," *Thermal Science*, vol. 17, no. 2, pp. 497–508, 2013.

[21] C. Casarosa and A. Franco, "Thermodynamic optimization of the operative parameters for the heat recovery in combined power plants," *International Journal of Thermodynamics*, vol. 4, no. 1, pp. 43–52, 2001.

[22] M. Valdes, A. Rovira, and M. D. Duran, "Influence of the heat recovery steam generator design parameters on the thermoeconomic performances of combined cycle gas turbine power plants," *International journal of energy research*, vol. 28, no. 14, pp. 1243–1254, 2004.

[23] J. Kotowicz, Job, and Marcin, "The characteristics of ultramodern combined cycle power plants," *Energy*, vol. 92, pp. 197–211, 2015.

[24] E. Ito, I. Okada, K. Tsukagoshi, A. Muyama, and J. Masada, "Development of key technologies for the next generation gas turbine," *Proceedings of the ASME Turbo Expo, Montreal, Canada*, 2007.

[25] 2017. [Online]. Available: http://www.coolprop.org/dev/fluid_properties/PurePseudoPure.html#list-of-fluids

[26] R. Pavri and G. D. Moore, "Gas turbine emissions and control," *General Electric Report No. GER-4211*, 2001.

[27] R. Kehlhofer, *Combined-cycle gas and steam turbine power plants*. PennWell, 1999.

[28] F. Frass, R. Hofmann, and K. Ponweiser, *Principles of finned-tube heat exchanger design for enhanced heat transfer*. Inst. f. Thermodynamics and Energy Conversion, Vienna University of Technology, 2007.

[29] T. K. Ibrahim and M. Rahman, "Effects of isentropic efficiencies on the performance of combined cycle power plants," *International Journal of Automotive and Mechanical Engineering*, vol. 12, p. 2914, 2015.

[30] T. Srinivas, "Thermodynamic modelling and optimization of a multi-pressure heat recovery steam generator in combined power cycle," vol. 67, pp. 827–834, 2008.

[31] M. Sharma and O. Singh, "Parametric Evaluation of Heat Recovery Steam Generator (HRSG)," *Heat Transfer Asian Research*, vol. 43, no. 8, pp. 691–705, 2014.

[32] P. Chiesa and E. Macchi, "A thermodynamic analysis of different options to break 60% electric efficiency in combined cycle power plants," in *ASME Turbo Expo 2002: Power for Land, Sea, and Air*. American Society of Mechanical Engineers, 2002, pp. 987–1002.

[33] Grimison, "Correlation and utilization of new data on flow resistance and heat transfer for cross flow over tube banks," *Trans. ASME*, vol. 59, no. 583, 1937.

[34] C. Weir, "Estimating the performance of gas turbine heat-recovery boilers off-design," *Proceedings of the Institution of Mechanical Engineers, Part A: Power and Process Engineering*, vol. 202, no. 4, pp. 269–277, 1988.

[35] A. Behbahani-nia, M. Bagheri, and R. Bahrampoury, "Optimization of fire tube heat recovery steam generators for cogeneration plants through genetic algorithm," *Applied Thermal Engineering*, vol. 30, no. 16, pp. 2378–2385, 2010.

[36] V. Gnielinski, "New equations for heat and mass transfer in turbulent pipe and channel flow," *Int. Chem. Eng*, vol. 16, no. 2, pp. 359–368, 1976.

[37] V. Klimenko, "A generalized correlation for two-phase forced flow heat transfer, second assessment," *International journal of heat and mass transfer*, vol. 33, no. 10, pp. 2073–2088, 1990.

[38] M. S. Salamah, "Design of dual pressure heat recovery steam generator for combined power plants," 2011.

[39] J. I. Manassaldi, S. F. Mussati, and N. J. Scenna, "Optimal synthesis and design of Heat Recovery Steam Generation (HRSG) via mathematical programming," *Energy*, vol. 36, no. 1, pp. 475–485, 2011.

[40] D. Duran and S. Galindo, "Thermoeconomic study of ccgt plants," in *Towards a Cleaner Planet*. Springer, 2007, pp. 87–97.

[41] J. S. In and S. Y. Lee, "Optimization of heat recovery steam generator through exergy analysis for combined cycle gas turbine power plants," *International Journal of Energy Research*, vol. 32, no. 9, pp. 859–869, 2008.

[42] 2017. [Online]. Available: https://es.mathworks.com/help/optim/ug/fmincon.html?s_tid=doc_ta#inputarg_fun

[43] "Choosing the algorithm," 2017. [Online]. Available: https://es.mathworks.com/help/optim/ug/choosing-the-algorithm.html

[44] A. Bassily, "Modeling, numerical optimization, and irreversibility reduction of a triple-pressure reheat combined cycle," *Energy*, vol. 32, no. 5, pp. 778–794, 2007.

[45] S. Sanaye and M. Rezazadeh, "Transient thermal modelling of heat recovery steam generators in combined cycle power plants," *International journal of energy research*, vol. 31, no. 11, pp. 1047–1063, 2007.

[46] BP, "Natural Gas 2016 in review," accessed 2017-09-09. [Online]. Available: http://www.bp.com/en/global/corporate/energy-economics/statistical-review-of-world-energy/natural-gas.html

[47] V. Ganapathy *et al.*, "Heat-recovery steam generators: understand the basics," *Chemical engineering progress*, vol. 92, no. 8, pp. 32–45, 1996.

[48] J. Li, K. Wang, and L. Cheng, "Experiment and optimization of a new kind once-through heat recovery steam generator (hrsg) based on analysis of exergy and economy," *Applied Thermal Engineering*, vol. 120, pp. 402–415, 2017.

[49] D. Taler, "Experimental determination of correlations for average heat transfer coefficients in heat exchangers on both fluid sides," *Heat and Mass Transfer*, vol. 49, no. 8, pp. 1125–1139, 2013.

[50] A. Franco and N. Giannini, "A general method for the optimum design of heat recovery steam generators," *Energy*, vol. 31, no. 15, pp. 3342–3361, 2006.

A Annex

A.1 Code single pressure model

```
% Clear variables
clear all
clc

% Input data
AP=15; % Approach and pinch points
PP=15;

Mg=650; % Gas properties
T1g=783;
P1g=101.3e3;

T1s=323; % Steam properties
T6s=768;
P6s=60e5;
PDs_SH=0.08;
PDs_EV=0;
PDs_EC=0.25;
X5s=1;

Lt=15.3; % Geometric properties
do=0.053;
di=0.050;
St=0.06625;
Sl=0.06625;
Nc_SH=10;
Nc_EV=10;
Nc_EC=10;
Nr_SH=10;
Nr_EV=10;
Nr_EC=10;

eta_Brayton=0.35; % CC properties
eta_Rankine=0.44;

% Properties steam side
H6s=CoolProp.PropsSI('H', 'T',T6s,'P',P6s, 'Water');
P5s=P6s*(1+PDs_SH);
H5s=CoolProp.PropsSI('H', 'Q',X5s,'P',P5s, 'Water');
T5s=CoolProp.PropsSI('T', 'Q',X5s,'P',P5s, 'Water');
T3s=T5s;
T2s=T3s-AP;
P2s=P5s;
H2s=CoolProp.PropsSI('H', 'T',T2s,'P',P2s, 'Water');
P1s=P2s*(1+PDs_EC);
H1s=CoolProp.PropsSI('H', 'P',P1s,'T',T1s, 'Water');

```

```
% Properties gas side
CPg=CoolProp.PropsSI('CPMASS', 'T',T1g,'P',P1g, 'Air');
T3g=T3s+PP;

% Heat transfer
Ms=(Mg*CPg*(T1g-T3g)/(H6s-H2s));
T2g=T1g-(Ms*(H6s-H5s)/(Mg*CPg));
T4g=T3g-(Ms*(H2s-H1s)/(Mg*CPg));

Q_SH=Mg*CPg*(T1g-T2g);
Q_EV=Mg*CPg*(T2g-T3g);
Q_EC=Mg*CPg*(T3g-T4g);
Q_tot=Q_SH+Q_EV+Q_EC;

% UA values
F_SH=1;
F_EV=1;
F_EC=1;

TLm_SH=((T1g-T6s-T2g+T5s)/(log((T1g-T6s)/(T2g-T5s))));
UA_SH=Q_SH/F_SH/TLm_SH;

TLm_EV=((T2g-T5s-T3g+T3s)/(log((T2g-T5s)/(T3g-T3s))));
UA_EV=Q_EV/F_EV/TLm_EV;

TLm_EC=((T3g-T3s-T4g+T1s)/(log((T3g-T3s)/(T4g-T1s))));
UA_EC=Q_EC/F_EC/TLm_EC;

% Gas heat transfer coefficient
k_g=CoolProp.PropsSI('L', 'T',T1g,'P',P1g, 'Air');
Mu_g=CoolProp.PropsSI('V', 'T',T1g,'P',P1g, 'Air');
Pr_g=CoolProp.PropsSI('Prandtl', 'T',T1g,'P',P1g, 'Air');

Re_g=(St/(2*(Sl-do)))*(Mg*do)/((St-do)*Nr_SH*Lt*Mu_g);

C1=0.518;
m=0.5560;

Nu_g=1.13*C1*(Re_g^m)*Pr_g^(1/3);

h_g=Nu_g*k_g/do;

% Steam heat transfer coefficient
Tm_s_SH=(T6s+T5s)/2;
Pm_s_SH=(P6s+P5s)/2;
Tm_s_EC=(T2s+T1s)/2;
Pm_s_EC=(P2s+P1s)/2;
```

```
k_s_SH=CoolProp.PropsSI('L', 'T',Tm_s_SH,...
    'P',Pm_s_SH, 'Water');
k_s_EV=CoolProp.PropsSI('L', 'Q',X5s,...
    'P',P5s, 'Water');
k_s_EC=CoolProp.PropsSI('L', 'T',Tm_s_EC,...
    'P',Pm_s_EC, 'Water');

Mu_s_SH=CoolProp.PropsSI('V', 'T',Tm_s_SH,...
    'P',Pm_s_SH, 'Water');
Mu_s_EV=CoolProp.PropsSI('V', 'Q',X5s,...
    'P',P5s, 'Water');
Mu_s_EC=CoolProp.PropsSI('V', 'T',Tm_s_EC,...
    'P',Pm_s_EC, 'Water');

Pr_s_SH=CoolProp.PropsSI('Prandtl', 'T',Tm_s_SH,...
    'P',Pm_s_SH, 'Air');
Pr_s_EV=CoolProp.PropsSI('Prandtl', 'Q',X5s,...
    'P',P5s, 'Water');
Pr_s_EC=CoolProp.PropsSI('Prandtl', 'T',Tm_s_EC,...
    'P',Pm_s_EC, 'Air');

Rho_s_SH=CoolProp.PropsSI('D','T',Tm_s_SH,...
    'P',Pm_s_SH, 'Water');
Rho_s_EV=CoolProp.PropsSI('D', 'Q',X5s,...
    'P',P5s, 'Water');
Rho_s_EC=CoolProp.PropsSI('D', 'T',Tm_s_EC,...
    'P',Pm_s_EC, 'Water');

Re_s_SH=(Ms)/(Nc_SH*Nr_SH*di*pi*Mu_s_SH*4);
Re_s_EV=(Ms)/(Nc_EV*Nr_EV*di*pi*Mu_s_EV*4);
Re_s_EC=(Ms)/(Nc_EC*Nr_EC*di*pi*Mu_s_EC*4);

f_s_SH=(0.79*log(Re_s_SH)-1.64)^-2;
f_s_EV=(0.79*log(Re_s_EV)-1.64)^-2;
f_s_EC=(0.79*log(Re_s_EC)-1.64)^-2;

Nu_s_SH=((f_s_SH/8)*(Re_s_SH-1000)*Pr_s_SH)/(1+12.7*...
    (f_s_SH/8)^0.5*(Pr_s_SH^(2/3)-1));
Nu_s_EV=((f_s_EV/8)*(Re_s_EV-1000)*Pr_s_EV)/(1+12.7*...
    (f_s_EV/8)^0.5*(Pr_s_EV^(2/3)-1));
Nu_s_EC=((f_s_EC/8)*(Re_s_EC-1000)*Pr_s_EC)/(1+12.7*...
    (f_s_EC/8)^0.5*(Pr_s_EC^(2/3)-1));

h_s_SH=Nu_s_SH*k_s_SH/di;
h_s_EV=Nu_s_EV*k_s_EV/di;
h_s_EC=Nu_s_EC*k_s_EC/di;

% Pressure drop water side (PDs)
vs_SH=Re_s_SH*Mu_s_SH/Rho_s_SH/di;
vs_EC=Re_s_EC*Mu_s_EC/Rho_s_EC/di;

```

```
PDs_SH=1/2*Rho_s_SH*vs_SH^2*f_s_SH*Lt/di;
PDs_EC=1/2*Rho_s_EC*vs_EC^2*f_s_EC*Lt/di;

Percentage_PD_SH=PDs_SH/P6s*100;
Percentage_PD_EC=PDs_EC/P6s*100;

% Global heat transfer coefficient
U_g_SH=(do/(h_s_SH*di)+1/h_g)^-1;
U_g_EV=(do/(h_s_EV*di)+1/h_g)^-1;
U_g_EC=(do/(h_s_EC*di)+1/h_g)^-1;

U_s_SH=(di/(h_g*do)+1/h_s_SH)^-1;
U_s_EV=(di/(h_g*do)+1/h_s_EV)^-1;
U_s_EC=(di/(h_g*do)+1/h_s_EC)^-1;

% Area
A_g_SH=UA_SH/U_g_SH;
A_g_EV=UA_EV/U_g_EV;
A_g_EC=UA_EC/U_g_EC;

A_s_SH=UA_SH/U_s_SH;
A_s_EV=UA_EV/U_s_EV;
A_s_EC=UA_EC/U_s_EC;

A_g=A_g_SH+A_g_EV+A_g_EC;
A_s=A_s_SH+A_s_EV+A_s_EC;

epsilon_HRSG=(Q_tot)/(Mg*CPg*(T1g-T1s));
eta_CC=eta_Brayton+epsilon_HRSG*eta_Rankine*(1-eta_Brayton);
```

A.2 Code optimization single pressure model

```
% Clear variables
clear all
clc

% Optimization parameters
A = [];
b = [];
Aeq = [];
beq = [];
nonlcon = [];

x0 = [15,15,15.3,10,10,10,10,10,10];
lb = [5,5,10,4,4,4,4,4,4];
ub = [25,20,20,12,12,12,12,12,12];

% Optimization

options = optimoptions('fmincon','Display','notify',...
    'Algorithm','active-set','PlotFcn',@Opti_PlotFvalue_1P);

[x,fval,exitflag,output] = fmincon(@Opti_Fun,x0,A,b,...
    Aeq,beq,lb,ub,nonlcon,options);

% Function input

function f = Opti_Fun(x)

% Input data

% Gas properties
Mg=650;
T1g=783;
P1g=101.3e3;
...
% Rest of the code
...
f=A_g;
end
```

A.3 Code multi pressure model

```
% Clear variables
clear all
clc

% Input data
AP_HP=25; % Approach and pinch points
PP_HP=20;
AP_IP=25;
PP_IP=20;
AP_LP=25;
PP_LP=20;
TTD=25;

Mg=650; % Gas properties
T1g=886;
P1g=101.3e3;

T20s=798; % Steam properties
T15s=525;
T9s=420;
T3s=323;
P20s=200e5;
P14s=8e5;
P8s=2e5;
PDs_SH=0.08;
PDs_EV=0;
PDs_EC=0.25;
X19s=1;
X13s=1;
X7s=1;

Lt=10; % Geometric properties
do=0.053;
di=0.050;
St=0.06625;
Sl=0.06625;
Nc_SH_HP=4;
Nc_EV_HP=4;
Nc_EC_HP=4;
Nr_SH_HP=4;
Nr_EV_HP=4;
Nr_EC_HP=4;
Nc_SH_IP=4;
Nc_EV_IP=4;
Nc_EC_IP=4;
Nr_SH_IP=4;
Nr_EV_IP=4;
Nr_EC_IP=4;
Nc_SH_LP=4;
```

```
Nc_EV_LP=4;
Nc_EC_LP=4;
Nr_SH_LP=4;
Nr_EV_LP=4;
Nr_EC_LP=4;

eta_Brayton=0.35; % CC properties
eta_Rankine=0.44;

% Properties HP steam side
H20s=CoolProp.PropsSI('H','T',T20s,'P',P20s,'Water');
P19s=P20s*(1+PDs_SH);
H19s=CoolProp.PropsSI('H','Q',X19s,'P',P19s,'Water');
T19s=CoolProp.PropsSI('T','Q',X19s,'P',P19s,'Water');
T17s=T19s;
T16s=T17s-AP_HP;
P16s=P19s;
H16s=CoolProp.PropsSI('H','T',T16s,'P',P16s,'Water');
P15s=P16s*(1+PDs_EC);
H15s=CoolProp.PropsSI('H','P',P15s,'T',T15s,'Water');

% Properties HP gas side
CPg_HP=CoolProp.PropsSI('CPMASS','T',T1g,'P',P1g,'Air');
T3g=T17s+PP_HP;

% Heat transfer HP
Ms_HP=(Mg*CPg_HP*(T1g-T3g)/(H20s-H16s));
T2g=T1g-(Ms_HP*(H20s-H19s)/(Mg*CPg_HP));
T4g=T3g-(Ms_HP*(H16s-H15s)/(Mg*CPg_HP));

Q_SH_HP=Mg*CPg_HP*(T1g-T2g);
Q_EV_HP=Mg*CPg_HP*(T2g-T3g);
Q_EC_HP=Mg*CPg_HP*(T3g-T4g);
Q_HP=Q_SH_HP+Q_EV_HP+Q_EC_HP;

% UA values HP
F_SH_HP=1;
F_EV_HP=1;
F_EC_HP=1;

TLm_SH_HP=((T1g-T20s-T2g+T19s)/(log((T1g-T20s)/(T2g-T19s))));
UA_SH_HP=Q_SH_HP/F_SH_HP/TLm_SH_HP;

TLm_EV_HP=((T2g-T19s-T3g+T17s)/(log((T2g-T19s)/(T3g-T17s))));
UA_EV_HP=Q_EV_HP/F_EV_HP/TLm_EV_HP;

TLm_EC_HP=((T3g-T17s-T4g+T15s)/(log((T3g-T17s)/(T4g-T15s))));
UA_EC_HP=Q_EC_HP/F_EC_HP/TLm_EC_HP;
```

```
% Gas heat transfer coefficient HP
k_g_HP=CoolProp.PropsSI('L','T',T1g,'P',P1g,'Air');
Mu_g_HP=CoolProp.PropsSI('V','T',T1g,'P',P1g,'Air');
Pr_g_HP=CoolProp.PropsSI('Prandtl','T',T1g,'P',P1g,'Air');
Rho_g_HP=CoolProp.PropsSI('D','T',T1g,'P',P1g,'Air');

Re_g_HP=(St/(2*(Sl-do)))*(Mg*do)/((St-do)*Nr_SH_HP*...
    Lt*Mu_g_HP);

C1_HP=0.518;
m_HP=0.5560;

Nu_g_HP=1.13*C1_HP*(Re_g_HP^m_HP)*Pr_g_HP^(1/3);

h_g_HP=Nu_g_HP*k_g_HP/do;

% Pressure drop gas side (PDg)

f_g_HP=0.2;
X_HP=1;

vg_HP=Re_g_HP*Mu_g_HP/Rho_g_HP/do;

PDg_HP=(Nr_SH_HP+Nr_EV_HP+Nr_EC_HP)*X_HP*1/2*...
    Rho_g_HP*vg_HP^2*f_g_HP;

P4g=P1g+PDg_HP;

% Steam heat transfer coefficient HP
Tm_s_SH_HP=(T20s+T19s)/2;
Pm_s_SH_HP=(P20s+P19s)/2;
Tm_s_EV_HP=(T16s+T19s)/2;
Tm_s_EC_HP=(T16s+T15s)/2;
Pm_s_EC_HP=(P16s+P15s)/2;

k_s_SH_HP=CoolProp.PropsSI('L','T',Tm_s_SH_HP,...
   'P',Pm_s_SH_HP,'Water');
k_s_EV_HP=CoolProp.PropsSI('L','Q',X19s,...
   'P',P19s,'Water');
k_s_EC_HP=CoolProp.PropsSI('L','T',Tm_s_EC_HP,...
   'P',Pm_s_EC_HP,'Water');

Mu_s_SH_HP=CoolProp.PropsSI('V','T',Tm_s_SH_HP,...
   'P',Pm_s_SH_HP,'Water');
Mu_s_EV_HP=CoolProp.PropsSI('V','Q',X19s,...
   'P',P19s,'Water');
Mu_s_EC_HP=CoolProp.PropsSI('V','T',Tm_s_EC_HP,...
   'P',Pm_s_EC_HP,'Water');

Pr_s_SH_HP=CoolProp.PropsSI('Prandtl','T',Tm_s_SH_HP,...
   'P',Pm_s_SH_HP,'Water');
```

```
Pr_s_EV_HP=CoolProp.PropsSI('Prandtl','Q',X19s,...
    'P',P19s,'Water');
Pr_s_EC_HP=CoolProp.PropsSI('Prandtl','T',Tm_s_EC_HP,...
    'P',Pm_s_EC_HP,'Water');

Rho_s_SH_HP=CoolProp.PropsSI('D','T',Tm_s_SH_HP,...
    'P',Pm_s_SH_HP,'Water');
Rho_s_EV_HP=CoolProp.PropsSI('D','Q',X19s,...
    'P',P19s,'Water');
Rho_s_EC_HP=CoolProp.PropsSI('D','T',Tm_s_EC_HP,...
    'P',Pm_s_EC_HP,'Water');

Re_s_SH_HP=(Ms_HP)/(Nc_SH_HP*Nr_SH_HP*di*pi*Mu_s_SH_HP*4);
Re_s_EV_HP=(Ms_HP)/(Nc_EV_HP*Nr_EV_HP*di*pi*Mu_s_EV_HP*4);
Re_s_EC_HP=(Ms_HP)/(Nc_EC_HP*Nr_EC_HP*di*pi*Mu_s_EC_HP*4);

f_s_SH_HP=(0.79*log(Re_s_SH_HP)-1.64)^-2;
f_s_EV_HP=(0.79*log(Re_s_EV_HP)-1.64)^-2;
f_s_EC_HP=(0.79*log(Re_s_EC_HP)-1.64)^-2;

Nu_s_SH_HP=((f_s_SH_HP/8)*(Re_s_SH_HP-1000)*Pr_s_SH_HP)/...
    (1+12.7*(f_s_SH_HP/8)^0.5*(Pr_s_SH_HP^(2/3)-1));
Nu_s_EV_HP=((f_s_EV_HP/8)*(Re_s_EV_HP-1000)*Pr_s_EV_HP)...
    /(1+12.7*(f_s_EV_HP/8)^0.5*(Pr_s_EV_HP^(2/3)-1));
Nu_s_EC_HP=((f_s_EC_HP/8)*(Re_s_EC_HP-1000)*Pr_s_EC_HP)...
    /(1+12.7*(f_s_EC_HP/8)^0.5*(Pr_s_EC_HP^(2/3)-1));

h_s_SH_HP=Nu_s_SH_HP*k_s_SH_HP/di;
h_s_EV_HP=Nu_s_EV_HP*k_s_EV_HP/di;
h_s_EC_HP=Nu_s_EC_HP*k_s_EC_HP/di;

% Pressure drop water side HP
vs_SH_HP=Re_s_SH_HP*Mu_s_SH_HP/Rho_s_SH_HP/di;
vs_EC_HP=Re_s_EC_HP*Mu_s_EC_HP/Rho_s_EC_HP/di;

PDs_SH_HP_Check=1/2*Rho_s_SH_HP*vs_SH_HP^2*f_s_SH_HP*Lt/di;
PDs_EC_HP_Check=1/2*Rho_s_EC_HP*vs_EC_HP^2*f_s_EC_HP*Lt/di;

Percentage_PD_SH_HP=PDs_SH_HP_Check/P20s*100;
Percentage_PD_EC_HP=PDs_EC_HP_Check/P20s*100;

% Global heat transfer coefficient HP
U_g_SH_HP=(do/(h_s_SH_HP*di)+1/h_g_HP)^-1;
U_g_EV_HP=(do/(h_s_EV_HP*di)+1/h_g_HP)^-1;
U_g_EC_HP=(do/(h_s_EC_HP*di)+1/h_g_HP)^-1;

U_s_SH_HP=(di/(h_g_HP*do)+1/h_s_SH_HP)^-1;
U_s_EV_HP=(di/(h_g_HP*do)+1/h_s_EV_HP)^-1;
U_s_EC_HP=(di/(h_g_HP*do)+1/h_s_EC_HP)^-1;
```

```
% Area HP
A_g_SH_HP=UA_SH_HP/U_g_SH_HP;
A_g_EV_HP=UA_EV_HP/U_g_EV_HP;
A_g_EC_HP=UA_EC_HP/U_g_EC_HP;

A_s_SH_HP=UA_SH_HP/U_s_SH_HP;
A_s_EV_HP=UA_EV_HP/U_s_EV_HP;
A_s_EC_HP=UA_EC_HP/U_s_EC_HP;

A_g_HP=A_g_SH_HP+A_g_EV_HP+A_g_EC_HP;
A_s_HP=A_s_SH_HP+A_s_EV_HP+A_s_EC_HP;

epsilon_HRSG_HP=(Q_HP)/(Mg*CPg_HP*(T1g-T15s));

% Properties IP steam side
T14s=T4g-TTD;
H14s=CoolProp.PropsSI('H','T',T14s,'P',P14s,'Water');
P13s=P14s*(1+PDs_SH);
H13s=CoolProp.PropsSI('H','Q',X13s,'P',P13s,'Water');
T13s=CoolProp.PropsSI('T','Q',X13s,'P',P13s,'Water');
T11s=T13s;
T10s=T13s-AP_IP;
P10s=P13s;
H10s=CoolProp.PropsSI('H','T',T10s,'P',P10s,'Water');
P9s=P10s*(1+PDs_EC);
H9s=CoolProp.PropsSI('H','P',P9s,'T',T9s,'Water');

% Properties IP gas side
CPg_IP=CoolProp.PropsSI('CPMASS','T',T4g,'P',P4g,'Air');
T6g=T11s+PP_IP;

% Heat transfer IP
Ms_IP=(Mg*CPg_IP*(T4g-T6g)/(H14s-H10s));
T5g=T4g-(Ms_IP*(H14s-H13s)/(Mg*CPg_IP));
T7g=T6g-(Ms_IP*(H10s-H9s)/(Mg*CPg_IP));

Q_SH_IP=Mg*CPg_IP*(T4g-T5g);
Q_EV_IP=Mg*CPg_IP*(T5g-T6g);
Q_EC_IP=Mg*CPg_IP*(T6g-T7g);
Q_IP=Q_SH_IP+Q_EV_IP+Q_EC_IP;

% UA coeficcients IP
F_SH_IP=1;
F_EV_IP=1;
F_EC_IP=1;

TLm_SH_IP=((T4g-T14s-T5g+T13s)/(log((T4g-T14s)/(T5g-T13s))));
UA_SH_IP=Q_SH_IP/F_SH_IP/TLm_SH_IP;

TLm_EV_IP=((T5g-T13s-T6g+T11s)/(log((T5g-T13s)/(T6g-T11s))));
UA_EV_IP=Q_EV_IP/F_EV_IP/TLm_EV_IP;
```

```
TLm_EC_IP=((T6g-T11s-T7g+T9s)/(log((T6g-T11s)/(T7g-T9s))));
UA_EC_IP=Q_EC_IP/F_EC_IP/TLm_EC_IP;

% Gas heat transfer coefficient IP
k_g_IP=CoolProp.PropsSI('L','T',T4g,'P',P4g,'Air');
Mu_g_IP=CoolProp.PropsSI('V','T',T4g,'P',P4g,'Air');
Pr_g_IP=CoolProp.PropsSI('Prandtl','T',T4g,'P',P4g,'Air');
Rho_g_IP=CoolProp.PropsSI('D','T',T4g,'P',P4g,'Air');

Re_g_IP=(St/(2*(Sl-do)))*(Mg*do)/((St-do)*Nr_SH_IP*...
    Lt*Mu_g_IP);

C1_IP=0.518;
m_IP=0.5560;

Nu_g_IP=1.13*C1_IP*(Re_g_IP^m_IP)*Pr_g_IP^(1/3);

h_g_IP=Nu_g_IP*k_g_IP/do;

% Pressure drop gas side (PDg)

f_g_IP=0.2;
X_IP=1;

vg_IP=Re_g_IP*Mu_g_IP/Rho_g_IP/do;

PDg_IP=(Nr_SH_IP+Nr_EV_IP+Nr_EC_IP)*X_IP*1/2*...
    Rho_g_IP*vg_IP^2*f_g_IP;

P7g=P4g+PDg_IP;

% Steam heat transfer coefficient IP
Tm_s_SH_IP=(T14s+T13s)/2;
Pm_s_SH_IP=(P14s+P13s)/2;
Tm_s_EC_IP=(T10s+T9s)/2;
Pm_s_EC_IP=(P10s+P9s)/2;

k_s_SH_IP=CoolProp.PropsSI('L','T',Tm_s_SH_IP,...
    'P',Pm_s_SH_IP,'Water');
k_s_EV_IP=CoolProp.PropsSI('L','Q',X13s,...
    'P',P13s,'Water');
k_s_EC_IP=CoolProp.PropsSI('L','T',Tm_s_EC_IP,...
    'P',Pm_s_EC_IP,'Water');

Mu_s_SH_IP=CoolProp.PropsSI('V','T',Tm_s_SH_IP,...
    'P',Pm_s_SH_IP,'Water');
Mu_s_EV_IP=CoolProp.PropsSI('V','Q',X13s,...
    'P',P13s,'Water');
Mu_s_EC_IP=CoolProp.PropsSI('V','T',Tm_s_EC_IP,...
    'P',Pm_s_EC_IP,'Water');

```

```
Pr_s_SH_IP=CoolProp.PropsSI('Prandtl','T',Tm_s_SH_IP,...
    'P',Pm_s_SH_IP,'Water');
Pr_s_EV_IP=CoolProp.PropsSI('Prandtl','Q',X13s,...
    'P',P13s,'Water');
Pr_s_EC_IP=CoolProp.PropsSI('Prandtl','T',Tm_s_EC_IP,...
    'P',Pm_s_EC_IP,'Water');

Rho_s_SH_IP=CoolProp.PropsSI('D','T',Tm_s_SH_IP,...
    'P',Pm_s_SH_IP,'Water');
Rho_s_EV_IP=CoolProp.PropsSI('D','Q',X13s,...
    'P',P13s,'Water');
Rho_s_EC_IP=CoolProp.PropsSI('D','T',Tm_s_EC_IP,...
    'P',Pm_s_EC_IP,'Water');

Re_s_SH_IP=(Ms_IP)/(Nc_SH_IP*Nr_SH_IP*di*pi*Mu_s_SH_IP*4);
Re_s_EV_IP=(Ms_IP)/(Nc_EV_IP*Nr_EV_IP*di*pi*Mu_s_EV_IP*4);
Re_s_EC_IP=(Ms_IP)/(Nc_EC_IP*Nr_EC_IP*di*pi*Mu_s_EC_IP*4);

f_s_SH_IP=(0.79*log(Re_s_SH_IP)-1.64)^-2;
f_s_EV_IP=(0.79*log(Re_s_EV_IP)-1.64)^-2;
f_s_EC_IP=(0.79*log(Re_s_EC_IP)-1.64)^-2;

Nu_s_SH_IP=((f_s_SH_IP/8)*(Re_s_SH_IP-1000)*Pr_s_SH_IP)/...
    (1+12.7*(f_s_SH_IP/8)^0.5*(Pr_s_SH_IP^(2/3)-1));
Nu_s_EV_IP=((f_s_EV_IP/8)*(Re_s_EV_IP-1000)*Pr_s_EV_IP)/...
    (1+12.7*(f_s_EV_IP/8)^0.5*(Pr_s_EV_IP^(2/3)-1));
Nu_s_EC_IP=((f_s_EC_IP/8)*(Re_s_EC_IP-1000)*Pr_s_EC_IP)/...
    (1+12.7*(f_s_EC_IP/8)^0.5*(Pr_s_EC_IP^(2/3)-1));

h_s_SH_IP=Nu_s_SH_IP*k_s_SH_IP/di;
h_s_EV_IP=Nu_s_EV_IP*k_s_EV_IP/di;
h_s_EC_IP=Nu_s_EC_IP*k_s_EC_IP/di;

% Pressure drop water side IP
vs_SH_IP=Re_s_SH_IP*Mu_s_SH_IP/Rho_s_SH_IP/di;
vs_EC_IP=Re_s_EC_IP*Mu_s_EC_IP/Rho_s_EC_IP/di;

PDs_SH_IP_Check=1/2*Rho_s_SH_IP*vs_SH_IP^2*f_s_SH_IP*Lt/di;
PDs_EC_IP_Check=1/2*Rho_s_EC_IP*vs_EC_IP^2*f_s_EC_IP*Lt/di;

Percentage_PD_SH_IP=PDs_SH_IP_Check/P20s*100;
Percentage_PD_EC_IP=PDs_EC_IP_Check/P20s*100;

% Global heat transfer coefficient IP
U_g_SH_IP=(do/(h_s_SH_IP*di)+1/h_g_IP)^-1;
U_g_EV_IP=(do/(h_s_EV_IP*di)+1/h_g_IP)^-1;
U_g_EC_IP=(do/(h_s_EC_IP*di)+1/h_g_IP)^-1;

U_s_SH_IP=(di/(h_g_IP*do)+1/h_s_SH_IP)^-1;
U_s_EV_IP=(di/(h_g_IP*do)+1/h_s_EV_IP)^-1;
U_s_EC_IP=(di/(h_g_IP*do)+1/h_s_EC_IP)^-1;
```

```
% Area IP
A_g_SH_IP=UA_SH_IP/U_g_SH_IP;
A_g_EV_IP=UA_EV_IP/U_g_EV_IP;
A_g_EC_IP=UA_EC_IP/U_g_EC_IP;

A_s_SH_IP=UA_SH_IP/U_s_SH_IP;
A_s_EV_IP=UA_EV_IP/U_s_EV_IP;
A_s_EC_IP=UA_EC_IP/U_s_EC_IP;

A_g_IP=A_g_SH_IP+A_g_EV_IP+A_g_EC_IP;
A_s_IP=A_s_SH_IP+A_s_EV_IP+A_s_EC_IP;

epsilon_HRSG_IP=(Q_IP)/(Mg*CPg_IP*(T4g-T9s));

% Properties LP steam side
T8s=T7g-TTD;
H8s=CoolProp.PropsSI('H','T',T8s,'P',P8s,'Water');
P7s=P8s*(1+PDs_SH);
H7s=CoolProp.PropsSI('H','Q',X7s,'P',P7s,'Water');
T7s=CoolProp.PropsSI('T','Q',X7s,'P',P7s,'Water');
T5s=T7s;
T4s=T7s-AP_LP;
P4s=P7s;
H4s=CoolProp.PropsSI('H','T',T4s,'P',P4s,'Water');
P3s=P4s*(1+PDs_EC);
H3s=CoolProp.PropsSI('H','P',P3s,'T',T3s,'Water');

% Properties LP gas side
CPg_LP=CoolProp.PropsSI('CPMASS','T',T7g,'P',P7g,'Air');
T9g=T5s+PP_LP;

% Heat transfer LP
Ms_LP=(Mg*CPg_LP*(T7g-T9g)/(H8s-H4s));
T8g=T7g-(Ms_LP*(H8s-H7s)/(Mg*CPg_LP));
T10g=T9g-(Ms_LP*(H4s-H3s)/(Mg*CPg_LP));

Q_SH_LP=Mg*CPg_LP*(T7g-T8g);
Q_EV_LP=Mg*CPg_LP*(T8g-T9g);
Q_EC_LP=Mg*CPg_LP*(T9g-T10g);
Q_LP=Q_SH_LP+Q_EV_LP+Q_EC_LP;

% UA coeficcients LP
F_SH_LP=1;
F_EV_LP=1;
F_EC_LP=1;

TLm_SH_LP=((T7g-T8s-T8g+T7s)/(log((T7g-T8s)/(T8g-T7s))));
UA_SH_LP=Q_SH_LP/F_SH_LP/TLm_SH_LP;

TLm_EV_LP=((T8g-T7s-T9g+T5s)/(log((T8g-T7s)/(T9g-T5s))));
UA_EV_LP=Q_EV_LP/F_EV_LP/TLm_EV_LP;
```

```
TLm_EC_LP=((T9g-T5s-T10g+T3s)/(log((T9g-T5s)/(T10g-T3s))));
UA_EC_LP=Q_EC_LP/F_EC_LP/TLm_EC_LP;

% Gas heat transfer coefficient LP
k_g_LP=CoolProp.PropsSI('L','T',T4g,'P',P4g,'Air');
Mu_g_LP=CoolProp.PropsSI('V','T',T4g,'P',P4g,'Air');
Pr_g_LP=CoolProp.PropsSI('Prandtl','T',T4g,'P',P4g,'Air');
Rho_g_LP=CoolProp.PropsSI('D','T',T4g,'P',P4g,'Air');

Re_g_LP=(St/(2*(Sl-do)))*(Mg*do)/((St-do)*...
    Nr_SH_LP*Lt*Mu_g_LP);

C1_LP=0.518;
m_LP=0.5560;

Nu_g_LP=1.13*C1_LP*(Re_g_LP^m_LP)*Pr_g_LP^(1/3);

h_g_LP=Nu_g_LP*k_g_LP/do;

% Pressure drop gas side (PDg)

f_g_LP=0.2;
X_LP=1;

vg_LP=Re_g_LP*Mu_g_LP/Rho_g_LP/do;

PDg_LP=(Nr_SH_LP+Nr_EV_LP+Nr_EC_LP)*X_LP*1/2*...
    Rho_g_LP*vg_LP^2*f_g_LP;

P10g=P7g+PDg_LP;

% Steam heat transfer coefficient LP
Tm_s_SH_LP=(T8s+T7s)/2;
Pm_s_SH_LP=(P8s+P7s)/2;
Tm_s_EC_LP=(T4s+T3s)/2;
Pm_s_EC_LP=(P4s+P3s)/2;

k_s_SH_LP=CoolProp.PropsSI('L','T',Tm_s_SH_LP,...
   'P',Pm_s_SH_LP,'Water');
k_s_EV_LP=CoolProp.PropsSI('L','Q',X7s,...
   'P',P7s,'Water');
k_s_EC_LP=CoolProp.PropsSI('L','T',Tm_s_EC_LP,...
    'P',Pm_s_EC_LP,'Water');

Mu_s_SH_LP=CoolProp.PropsSI('V','T',Tm_s_SH_LP,...
   'P',Pm_s_SH_LP,'Water');
Mu_s_EV_LP=CoolProp.PropsSI('V','Q',X7s,...
   'P',P7s,'Water');
Mu_s_EC_LP=CoolProp.PropsSI('V','T',Tm_s_EC_LP,...
   'P',Pm_s_EC_LP,'Water');

```

```
458 Pr_s_SH_LP=CoolProp.PropsSI('Prandtl','T',Tm_s_SH_LP,...
459     'P',Pm_s_SH_LP,'Water');
460 Pr_s_EV_LP=CoolProp.PropsSI('Prandtl','Q',X7s,...
461     'P',P7s,'Water');
462 Pr_s_EC_LP=CoolProp.PropsSI('Prandtl','T',Tm_s_EC_LP,...
463     'P',Pm_s_EC_LP,'Water');
464
465 Rho_s_SH_LP=CoolProp.PropsSI('D','T',Tm_s_SH_LP,...
466     'P',Pm_s_SH_LP,'Water');
467 Rho_s_EV_LP=CoolProp.PropsSI('D','Q',X7s,...
468     'P',P7s,'Water');
469 Rho_s_EC_LP=CoolProp.PropsSI('D','T',Tm_s_EC_LP,...
470     'P',Pm_s_EC_LP,'Water');
471
472 Re_s_SH_LP=(Ms_LP)/(Nc_SH_LP*Nr_SH_LP*di*pi*Mu_s_SH_LP*4);
473 Re_s_EV_LP=(Ms_LP)/(Nc_EV_LP*Nr_EV_LP*di*pi*Mu_s_EV_LP*4);
474 Re_s_EC_LP=(Ms_LP)/(Nc_EC_LP*Nr_EC_LP*di*pi*Mu_s_EC_LP*4);
475
476 f_s_SH_LP=(0.79*log(Re_s_SH_LP)-1.64)^-2;
477 f_s_EV_LP=(0.79*log(Re_s_EV_LP)-1.64)^-2;
478 f_s_EC_LP=(0.79*log(Re_s_EC_LP)-1.64)^-2;
479
480 Nu_s_SH_LP=((f_s_SH_LP/8)*(Re_s_SH_LP-1000)*Pr_s_SH_LP)/...
481     (1+12.7*(f_s_SH_LP/8)^0.5*(Pr_s_SH_LP^(2/3)-1));
482 Nu_s_EV_LP=((f_s_EV_LP/8)*(Re_s_EV_LP-1000)*Pr_s_EV_LP)/...
483     (1+12.7*(f_s_EV_LP/8)^0.5*(Pr_s_EV_LP^(2/3)-1));
484 Nu_s_EC_LP=((f_s_EC_LP/8)*(Re_s_EC_LP-1000)*Pr_s_EC_LP)/...
485     (1+12.7*(f_s_EC_LP/8)^0.5*(Pr_s_EC_LP^(2/3)-1));
486
487 h_s_SH_LP=Nu_s_SH_LP*k_s_SH_LP/di;
488 h_s_EV_LP=Nu_s_EV_LP*k_s_EV_LP/di;
489 h_s_EC_LP=Nu_s_EC_LP*k_s_EC_LP/di;
490
491 % Pressure drop water side LP
492 vs_SH_LP=Re_s_SH_LP*Mu_s_SH_LP/Rho_s_SH_LP/di;
493 vs_EC_LP=Re_s_EC_LP*Mu_s_EC_LP/Rho_s_EC_LP/di;
494
495 PDs_SH_LP_Check=1/2*Rho_s_SH_LP*vs_SH_LP^2*f_s_SH_LP*Lt/di;
496 PDs_EC_LP_Check=1/2*Rho_s_EC_LP*vs_EC_LP^2*f_s_EC_LP*Lt/di;
497
498 Percentage_PD_SH_LP=PDs_SH_LP_Check/P20s*100;
499 Percentage_PD_EC_LP=PDs_EC_LP_Check/P20s*100;
500
501 % Global heat transfer coefficient LP
502 U_g_SH_LP=(do/(h_s_SH_LP*di)+1/h_g_LP)^-1;
503 U_g_EV_LP=(do/(h_s_EV_LP*di)+1/h_g_LP)^-1;
504 U_g_EC_LP=(do/(h_s_EC_LP*di)+1/h_g_LP)^-1;
505
506 U_s_SH_LP=(di/(h_g_LP*do)+1/h_s_SH_LP)^-1;
507 U_s_EV_LP=(di/(h_g_LP*do)+1/h_s_EV_LP)^-1;
508 U_s_EC_LP=(di/(h_g_LP*do)+1/h_s_EC_LP)^-1;
```

```
% Area LP
A_g_SH_LP=UA_SH_LP/U_g_SH_LP;
A_g_EV_LP=UA_EV_LP/U_g_EV_LP;
A_g_EC_LP=UA_EC_LP/U_g_EC_LP;

A_s_SH_LP=UA_SH_LP/U_s_SH_LP;
A_s_EV_LP=UA_EV_LP/U_s_EV_LP;
A_s_EC_LP=UA_EC_LP/U_s_EC_LP;

A_g_LP=A_g_SH_LP+A_g_EV_LP+A_g_EC_LP;
A_s_LP=A_s_SH_LP+A_s_EV_LP+A_s_EC_LP;

epsilon_HRSG_LP=(Q_LP)/(Mg*CPg_LP*(T7g-T3s));

% Total CC
Q_tot=Q_HP+Q_IP+Q_LP;
A_g_tot=A_g_HP+A_g_IP+A_g_LP;
A_s_tot=A_s_HP+A_s_IP+A_s_LP;
epsilon_HRSG=(Q_tot)/(Mg*CPg_HP*(T1g-T3s));
eta_CC=eta_Brayton+epsilon_HRSG*eta_Rankine*(1-eta_Brayton);
```